



Measurement of the Higgs boson mass in the $H \rightarrow ZZ^* \rightarrow 4\ell$ and $H \rightarrow \gamma\gamma$ channels with $\sqrt{s} = 13$ TeV pp collisions using the ATLAS detector

The ATLAS Collaboration ^{*}

ARTICLE INFO

Article history:

Received 4 June 2018

Received in revised form 20 July 2018

Accepted 27 July 2018

Available online 2 August 2018

Editor: M. Doser

ABSTRACT

The mass of the Higgs boson is measured in the $H \rightarrow ZZ^* \rightarrow 4\ell$ and in the $H \rightarrow \gamma\gamma$ decay channels with 36.1 fb^{-1} of proton–proton collision data from the Large Hadron Collider at a centre-of-mass energy of 13 TeV recorded by the ATLAS detector in 2015 and 2016. The measured value in the $H \rightarrow ZZ^* \rightarrow 4\ell$ channel is $m_H^{ZZ^*} = 124.79 \pm 0.37 \text{ GeV}$, while the measured value in the $H \rightarrow \gamma\gamma$ channel is $m_H^{\gamma\gamma} = 124.93 \pm 0.40 \text{ GeV}$. Combining these results with the ATLAS measurement based on 7 and 8 TeV proton–proton collision data yields a Higgs boson mass of $m_H = 124.97 \pm 0.24 \text{ GeV}$.

© 2018 The Author. Published by Elsevier B.V. This is an open access article under the CC BY license (<http://creativecommons.org/licenses/by/4.0/>). Funded by SCOAP³.

1. Introduction

The observation of a Higgs boson, H , by the ATLAS and CMS experiments [1,2] with the Large Hadron Collider (LHC) Run 1 proton–proton (pp) collision data at centre-of-mass energies of $\sqrt{s} = 7$ and 8 TeV was a major step towards understanding the mechanism of electroweak (EW) symmetry breaking [3–5]. The mass of the Higgs boson was measured to be $125.09 \pm 0.24 \text{ GeV}$ [6] based on the combined Run 1 data samples of the ATLAS and CMS Collaborations, who also reported individual mass measurements in Refs. [7,8]. Recently, the CMS Collaboration measured the Higgs boson mass in the $H \rightarrow ZZ^* \rightarrow 4\ell$ channel using 35.9 fb^{-1} of 13 TeV pp collision data [9]. The measured value of the mass is $125.26 \pm 0.21 \text{ GeV}$.

This Letter presents a measurement of the Higgs boson mass, m_H , with 36.1 fb^{-1} of $\sqrt{s} = 13$ TeV pp collision data recorded with the ATLAS detector. The measurement is derived from a combined fit to the four-lepton and diphoton invariant mass spectra in the decay channels $H \rightarrow ZZ^* \rightarrow 4\ell$ ($\ell = e, \mu$) and $H \rightarrow \gamma\gamma$. A combination with the ATLAS Run 1 data is also presented.

2. ATLAS detector

The ATLAS experiment [10] at the LHC is a multi-purpose particle detector with nearly 4π coverage in solid angle.¹ It consists

of an inner tracking detector (ID) surrounded by a 2 T superconducting solenoid, electromagnetic (EM) and hadronic calorimeters, and a muon spectrometer (MS) incorporating three large superconducting toroidal magnets. The ID provides tracking for charged particles for $|\eta| < 2.5$. The calorimeter system covers the pseudorapidity range $|\eta| < 4.9$. Its electromagnetic part is segmented into three shower-depth layers for $|\eta| < 2.5$ and includes a presampler for $|\eta| < 1.8$. The MS includes high-precision tracking chambers ($|\eta| < 2.7$) and fast trigger chambers ($|\eta| < 2.4$). Online event selection is performed by a first-level trigger with a maximum rate of 100 kHz, implemented in custom electronics, followed by a software-based high-level trigger with a maximum rate of 1 kHz.

3. Data and simulated samples

This measurement uses data from pp collisions with a centre-of-mass energy of 13 TeV collected during 2015 and 2016 using single-lepton, dilepton, trilepton and diphoton triggers, with looser identification, isolation and transverse momentum (p_T) requirements than those applied offline. The combined efficiency of the lepton triggers is about 98% for the $H \rightarrow ZZ^* \rightarrow 4\ell$ events (assuming $m_H = 125 \text{ GeV}$) passing the offline selection. The diphoton trigger efficiency is higher than 99% for selected $H \rightarrow \gamma\gamma$ events (assuming $m_H = 125 \text{ GeV}$). After trigger and data-quality requirements, the integrated luminosity of the data sample is 36.1 fb^{-1} .

^{*} E-mail address: atlas.publications@cern.ch.

¹ ATLAS uses a right-handed coordinate system with its origin at the nominal interaction point (IP) in the centre of the detector and the z -axis along the beam pipe. The x -axis points from the IP to the centre of the LHC ring, and the y -axis

points upwards. Cylindrical coordinates (r, ϕ) are used in the transverse plane, ϕ being the azimuthal angle around the z -axis. The pseudorapidity is defined in terms of the polar angle θ as $\eta = -\ln \tan(\theta/2)$. Angular distance is measured in units of $\Delta R \equiv \sqrt{(\Delta\eta)^2 + (\Delta\phi)^2}$.

The mean number of proton–proton interactions per bunch crossing (integrated luminosity) is 14 (3.2 fb^{-1}) in the 2015 data set and 25 (32.9 fb^{-1}) in the 2016 data set.

Monte Carlo (MC) simulation is used in the analysis to model the detector response for signal and background processes. For the $H \rightarrow ZZ^* \rightarrow 4\ell$ measurement, a detailed list and description of the MC-simulated samples used can be found in Ref. [11] and only a few differences specific to the mass analysis are mentioned here. For the gluon–gluon fusion (ggF) signal, the NNLOPS sample generated at next-to-next-to-leading order (NNLO) in QCD [12] with $m_H = 123, 125, 126 \text{ GeV}$ and the PDF4LHC NLO parton distribution function (PDF) set [13] was used. Additional samples generated at different m_H values (120, 122, 124, 125, 126, 128, 130 GeV) at next-to-leading order (NLO) were also used. The NLO ggF simulation was performed with PowHEG-Box v2 [14] interfaced to PYTHIA 8 [15] for parton showering and hadronisation, and to EVTGEN [16] for the simulation of b -hadron decays. The CT10NLO [17] PDF set was used for the hard process and the CTEQ6L1 [18] set for the parton shower. The non-perturbative effects were modelled using the AZNLO set of tuned parameters [19].

The ZZ^* continuum background from quark–antiquark annihilation was modelled at NLO in QCD using PowHEG-Box v2 and interfaced to PYTHIA 8 for parton showering and hadronisation, and to EVTGEN for b -hadron decays. The PDF set used is the same as for the NLO ggF signal. NNLO QCD [20,21] and NLO EW corrections [22,23] were applied as a function of the invariant mass of the ZZ^* system (m_{ZZ^*}).

For the $H \rightarrow \gamma\gamma$ measurement, the same $H \rightarrow \gamma\gamma$ signal (generated for $m_H = 125 \text{ GeV}$) and background simulated events used for the measurements of the Higgs boson couplings and fiducial cross-sections in the diphoton final state [24] were used. In addition, signal samples with alternative m_H values (110, 122, 123, 124, 126, 127, 130, 140 GeV) were produced, with the same generators and settings as the $m_H = 125 \text{ GeV}$ samples, but only for the four Higgs boson production modes with largest cross-section: gluon–gluon fusion, vector–boson fusion (VBF), and associated production with a vector boson $V = W, Z$ (VH), for $q\bar{q}' \rightarrow VH$ and $gg \rightarrow ZH$. For rarer processes, such as associated production of the Higgs boson with a top–quark pair ($t\bar{t}H$) or a single top–quark (tH), contributing to less than 2% of the total cross-section, only samples at $m_H = 125 \text{ GeV}$ were used.

Except for the $\gamma\gamma$ background sample, whose modelling requires a large MC sample obtained through a fast parametric simulation of the calorimeter response [25], the generated events for all processes were passed through a GEANT4 [26] simulation of the response of the ATLAS detector [25]. For both detector emulation methods, events were reconstructed with the same algorithms as the data. Additional proton–proton interactions (pile-up) were included in both the parametric and the GEANT4 simulations, matching the average number of interactions per LHC bunch crossing to the spectrum observed in the data.

The Standard Model (SM) expectations for the Higgs boson production cross-section times branching ratio, in the various production modes and final states under study and at each value of m_H , were taken from Refs. [27–30] and used to normalise the simulated samples, as described in Refs. [11,24].

4. Muon reconstruction, identification and calibration

Muon track reconstruction is first performed independently in the ID and the MS. Hit information from the individual subdetectors is then used in a combined muon reconstruction, which includes information from the calorimeters.

Corrections to the reconstructed momentum are applied in order to match the simulation to data precisely. These corrections

to the simulated momentum resolution and momentum scale are parameterised as a power expansion in the muon p_T , with each coefficient measured separately for the ID and MS, as a function of η and ϕ , from large data samples of $J/\psi \rightarrow \mu^+\mu^-$ and $Z \rightarrow \mu^+\mu^-$ decays. The scale corrections range from 0.1% to 0.5% for the p_T of muons originating from $J/\psi \rightarrow \mu^+\mu^-$ and $Z \rightarrow \mu^+\mu^-$ decays and account for inaccurate measurement of the energy lost in the traversed material, local magnetic field inaccuracies and geometrical distortions. The corrections to the muon momentum resolution for muons from $J/\psi \rightarrow \mu^+\mu^-$ and $Z \rightarrow \mu^+\mu^-$ are at the percent level. After detector alignment, there are residual local misalignments that bias the muon track sagitta, leaving the track χ^2 invariant [31,32], and introduce a small charge-dependent resolution degradation. The bias in the measured momentum of each muon is corrected by an iterative procedure derived from $Z \rightarrow \mu^+\mu^-$ decays and checked against the E/p ratio measured in $Z \rightarrow e^+e^-$ decays. The residual effect after correction is reduced to the per mille level at the scale of the Z boson mass. This correction improves the resolution of the dimuon invariant mass in Z boson decays by 1% to 5%, depending on η and ϕ of the muon. The systematic uncertainty associated with this correction is estimated for each muon using simulation and is found to be about 0.4×10^{-3} for the average momentum of muons from $Z \rightarrow \mu^+\mu^-$ decays.

For muons from $Z \rightarrow \mu^+\mu^-$ decays, with momenta of about 45 GeV, the momentum scale is determined to a precision of 0.05% for muons with $|\eta| < 2$, and about 0.2% for muons with $|\eta| \geq 2$. Similarly, the resolution is known with a precision ranging from 1% to 2% for muons with $|\eta| < 2$ and around 10% for muons with $|\eta| \geq 2$ [33]. Both the momentum scale and momentum resolution uncertainties in the corrections to simulation are taken as fully correlated between the Run 1 and Run 2 measurements.

5. Photon and electron reconstruction, identification and calibration

Photon and electron candidates are reconstructed from clusters of electromagnetic calorimeter cells [34]. Clusters without a matching track or reconstructed conversion vertex in the inner detector are classified as unconverted photons. Those with a matching reconstructed conversion vertex or a matching track, consistent with originating from a photon conversion, are classified as converted photons [35]. Clusters matched to a track consistent with originating from an electron (based on transition radiation in the ID) produced in the beam interaction region are considered electron candidates.

The energy measurement for reconstructed electrons and photons is performed by summing the energies measured in the EM calorimeter cells belonging to the candidate cluster. The energy is measured from a cluster size of $\Delta\eta \times \Delta\phi = 0.075 \times 0.175$ in the barrel region of the calorimeter and $\Delta\eta \times \Delta\phi = 0.125 \times 0.125$ in the calorimeter endcaps. The procedure for the energy measurement of electrons and photons closely follows that used in Run 1 [36], with updates to reflect the 2015 and 2016 data-taking conditions:

- The different layers of the electromagnetic calorimeter are intercalibrated by applying methods similar to those described in Ref. [36]. The first and second calorimeter layers are intercalibrated using the energy deposited by muons from $Z \rightarrow \mu^+\mu^-$ decays, with a typical uncertainty of 0.7% to 1.5% (1.5% to 2.5%) as a function of η in the barrel (endcap) calorimeter, for $|\eta| < 2.4$. This uncertainty is added in quadrature to the uncertainty in the modelling of the muon ionisation in the simulation (1% to 1.5% depending on η). The energy scale of the presampler is estimated using electrons from Z boson

decays, after correcting the simulation on the basis of the correlations between the amount of detector material and the ratio of the energies deposited in the first and second layers of the calorimeter. The uncertainty in the presampler energy scale varies between 1.5% and 3% depending on η .

- The cluster energy is corrected for energy loss in the inactive materials in front of the calorimeter, the fraction of energy deposited outside the area of the cluster in the η - ϕ plane, the amount of energy lost behind the electromagnetic calorimeter, and to account for the variation of the energy response as a function of the impact point in the calorimeter. The calibration coefficients used to apply these corrections are obtained from a detailed simulation of the detector response to electrons and photons, and are optimised with a boosted decision tree (BDT). The algorithm, described in Ref. [37], has been trained on simulated samples corresponding to the data-taking conditions of 2015 and 2016. The response is calibrated separately for electron candidates, converted photon candidates and unconverted photon candidates. In data, small corrections are applied for the ϕ -dependent energy loss in the gaps between the barrel calorimeter modules (corrections up to 2%, in about 5% of the calorimeter acceptance) and for inhomogeneities due to sectors operated at non-nominal high voltage (corrections between 1% and 7%, in about 2% of the calorimeter acceptance).
- The global calorimeter energy scale is determined in situ with a large sample of $Z \rightarrow e^+e^-$ events selected in the 2015 and 2016 datasets. The energy response in data and simulation is equalised by applying η -dependent correction factors to match the invariant mass distributions of $Z \rightarrow e^+e^-$ events. The uncertainty in these energy scale correction factors ranges from 0.02% to 0.1% as a function of η , except for the barrel-endcap transition region ($1.37 < |\eta| < 1.52$), where it reaches a few per mille. In this procedure, the simulated width of the reconstructed Z boson mass distribution is matched to the width observed in data by adding in the simulation a contribution to the constant term c of the electron energy resolution, $\frac{\sigma_E}{E} = \frac{a}{\sqrt{E}} \oplus \frac{b}{E} \oplus c$. This constant term varies between 0.7% and 2% for $|\eta| < 2.4$ with an uncertainty of 0.03%–0.3%, except for the barrel-endcap transition region, where the constant term is slightly higher (2.5%–2.9%) with an uncertainty reaching 0.6%.

The main sources of systematic uncertainties in the calibration procedure discussed in Ref. [36] have been revisited. These sources include uncertainties in the method used to extract the energy scale correction factors, as well as uncertainties due to the extrapolation of the energy scale from $Z \rightarrow e^+e^-$ events to photons, and also to electrons with energies different from those produced in $Z \rightarrow e^+e^-$ decays. The latter arise from the uncertainties in the linearity of the response due to the relative calibration of the different gains used in the calorimeter readout, in the knowledge of the material in front of the calorimeter (inside and outside of the ID, referred to as ID and non-ID material in the following), in the intercalibration of the different calorimeter layers, in the modelling of the lateral shower shapes and in the reconstruction of photon conversions. The total calibration uncertainty for photons with transverse energy (E_T) around 60 GeV is 0.2%–0.3% in the barrel and 0.45%–0.8% in the endcap. These uncertainties are close to those quoted in Ref. [36], but typically about 10% larger. The small increase in the uncertainty arises mostly from a larger uncertainty in the relative calibration of the first and second calorimeter layers with muons because of a worse ratio of signal to pile-up noise in Run 2 data. In the case of electrons with E_T around 40 GeV, the total uncertainty ranges between 0.03% and 0.2% in most of the detector acceptance. For electrons with E_T around 10 GeV the uncertainty ranges between 0.3% and 0.8%.

The accuracy of the energy calibration for low-energy electrons (5–20 GeV) is checked by computing residual energy calibration corrections (after applying the corrections extracted from the $Z \rightarrow e^+e^-$ sample) for an independent sample of $J/\psi \rightarrow e^+e^-$ events. These residual correction factors are found to be compatible with one within uncertainties. A similar check is performed by computing residual corrections for photons in a sample of radiative Z boson decays. They are found to be compatible with one within uncertainties which are given by the combination of the statistical uncertainty of the radiative Z boson decays sample and of the systematic uncertainty from the extrapolation of the energy scale from electrons to photons.

Systematic uncertainties in the calorimeter energy resolution arise from uncertainties in the modelling of the sampling term a/\sqrt{E} and in the measurement of the constant term in Z boson decays, in the amount of material in front of the calorimeter, which affects electrons and photons differently, and in the modelling of the contribution to the resolution from fluctuations in the pile-up from additional proton–proton interactions in the same or neighbouring bunch crossings. The uncertainty of the energy resolution for electrons and photons with transverse energy between 30 and 60 GeV varies between 5% and 10%.

The identification of photons and the rejection of background from hadrons is based primarily on shower shapes in the calorimeter. The two levels of selection, loose and tight, are described in Ref. [35]. To further reduce the background from jets, two complementary isolation selection criteria are used, based on topological clusters of energy deposits in the calorimeter and on reconstructed tracks in a direction close to that of the photon candidate, as described in Ref. [24].

Electrons are identified using a likelihood-based method combining information from the electromagnetic calorimeter and the ID. As in the case of photons, electrons are required to be isolated using both the calorimeter-based and track-based isolation variables as described in Ref. [38].

6. Statistical methods

The mass measurement is based on the maximisation of the profile likelihood ratio [39,40]

$$\Lambda(m_H) = \frac{L(m_H, \hat{\hat{\theta}}(m_H))}{L(\hat{m}_H, \hat{\theta})},$$

where the vectors $\hat{\theta}$ and \hat{m}_H denote the unconditional-maximum likelihood estimates of the parameters of the likelihood function L , while $\hat{\hat{\theta}}$ is the conditional maximum-likelihood estimate of the parameters θ for a fixed value of the parameter m_H . Systematic uncertainties and their correlations are modelled by introducing nuisance parameters θ described by likelihood functions associated with the estimate of the corresponding effect [6].

The statistical uncertainty of m_H is estimated by fixing all nuisance parameters to their best-fit values, all remaining parameters are thus left unconstrained. This approach yields a lower bound on the statistical uncertainty, when the combination of the different event categories discussed in the next sections is performed neglecting the different impact of the systematic uncertainties in each category. The upper bound on the total systematic uncertainty is estimated by subtracting in quadrature the statistical uncertainty from the total uncertainty.

Alternatively, the decomposition of the uncertainty into statistical and systematic components is performed using the BLUE method [41–43]. The two approaches may lead to different results from the decomposition of the uncertainty for a combination of

measurements with significant and uncorrelated systematic uncertainties.

7. Mass measurement in the $H \rightarrow ZZ^* \rightarrow 4\ell$ channel

7.1. Event selection

Events are required to contain at least four isolated leptons ($\ell = e, \mu$) that emerge from a common vertex, form two pairs of oppositely charged same-flavour leptons. Electrons are required to be within the full pseudorapidity range of the inner tracking detector ($|\eta| < 2.47$) and have transverse energy $E_T > 7$ GeV, while muons are required to be within the pseudorapidity range of the muon spectrometer ($|\eta| < 2.7$) and have transverse momentum $p_T > 5$ GeV. The three higher- p_T (E_T) leptons in each quadruplet are required to pass thresholds of 20, 15, and 10 GeV, respectively. A detailed description of the event selection can be found in Refs. [11,44].

The lepton pair with an invariant mass closest to the Z boson mass in each quadruplet is referred to as the leading dilepton pair, while the remaining pair is referred to as the subleading dilepton pair. The selected events are split according to the flavour of the leading and subleading pairs; ordered according to the expected selection efficiency, they are 4μ , $2e2\mu$, $2\mu2e$, $4e$. Reconstructed photon candidates passing final-state radiation selections are searched for in all the events [45]. Such photons are found in 4% of the events and their energy is included in the mass computation. In addition, a kinematic fit is performed to constrain the invariant mass of the leading lepton pair to the Z boson mass, improving the $m_{4\ell}$ resolution by about 15% [7]. The improvement brought by the correction of the local tracker misalignments, as discussed in Section 4, is at the percent level for the $m_{4\ell}$ resolution of signal events. After event selection, the $m_{4\ell}$ resolution for the signal (at $m_H = 125$ GeV), estimated with a Gaussian fit around the peak, is expected to be about 1.6, 1.8, 2.2 and 2.4 GeV for the 4μ , $2e2\mu$, $2\mu2e$ and $4e$ channels respectively. In the fit range of $110 < m_{4\ell} < 135$ GeV, 123 candidate events are observed. The yield is in agreement with an expectation of 107 ± 6 events, 53% of which are expected to be from the signal, assuming $m_H = 125$ GeV.

The dominant contribution to the background is non-resonant ZZ^* production (about 84% of the total background yield). Events with hadrons, or hadron decay products, misidentified as prompt leptons also contribute (about 15%). Events originating from $t\bar{t}+Z$, ZZZ , WZZ , and WWZ production are estimated to contribute less than 1% of the total background. The residual combinatorial background, originating from events with additional prompt leptons, was found to be negligibly small [44].

The precision of the mass measurement is further improved by categorising events with a multivariate discriminant which distinguishes the signal from the ZZ^* background. The BDT described in Ref. [7], based on the same input variables, is trained on simulated signal events with different mass values simultaneously (124, 125 and 126 GeV) and ZZ^* background events that pass the event selection. For each final state, four equal-size exclusive bins in the BDT response are used. This improves the precision of the m_H measurement in the 4ℓ decay channel by about 6%.

7.2. Signal and background model

The invariant mass in each category is described by the sum of a signal and a background distribution.

Non-resonant ZZ^* production is estimated using simulation normalised to the most accurate predictions and validated in the sidebands of the selected 4ℓ mass range. Smaller contributions to the background from $t\bar{t}+Z$, ZZZ , WZZ and WWZ production

are also estimated using simulation while the contributions from Z +jets, WZ , and $t\bar{t}$ production where one or more hadrons, or hadron decay products, are misidentified as a prompt lepton are estimated from data using minimal input from simulation following the methodology described in Ref. [11]. For each contribution to the background, the probability density function (pdf) is estimated with the kernel density estimation.

For the determination of the signal distribution, an approach based on the event-by-event response of the detector is employed. The measured $m_{4\ell}$ signal distribution is modelled as the convolution of a relativistic Breit–Wigner distribution, of 4.1 MeV width [27–30] and a peak at m_H , with a four-lepton invariant mass response distribution which is derived event-by-event from the expected response distributions of the individual leptons. The lepton energy response distributions are derived from simulation as a function of the lepton energy and detector region. The lepton energy response is modelled as a weighted sum of three Gaussian distributions. For an observed event, the $m_{4\ell}$ pdf is derived from the convolution of the response distributions of the four measured leptons. The direct convolution of the four leptons distributions, leading to $3^4 = 81$ Gaussian distributions, is simplified to a weighted sum of four Gaussian pdfs following an iterative merging procedure as performed with the Gaussian-sum filter procedure [46,47]. An additional correction is applied to remove the residual differences which arise from the correlation between the lepton energy measurements introduced by the kinematic constrained fit on the leading dilepton pair and the BDT categorisation of events. These are corrected by a fit of scaling modifiers of the reduced response parameters to the simulated four-lepton resolution. These modifiers are about 0.1% for the means and up to 10% for the widths of the Gaussians of the reduced response.

Finally, the mass of the Higgs boson m_H is determined by a simultaneous unbinned fit of signal-plus-background distributions to data over the sixteen categories.² The per-event component of the signal pdf is added to the background distribution which is integrated over all kinematic configurations of the four final state leptons. In each of the four BDT categories, the signal yield is factorised by a floating normalisation modifier independent for each BDT category. The measured Higgs boson mass depends on the lepton energy resolution and the lepton energy scale. Uncertainties in these quantities are accounted for in the fit by Gaussian-distributed penalty terms whose widths are obtained from auxiliary data or simulation control samples. The expected uncertainty, with $m_H = 125$ GeV and production rates predicted by the SM, for a data sample of the size of the experimental set, evaluated using simulation-based pseudo-experiments, is ± 0.35 GeV.

A validation with data is performed with $Z \rightarrow 4\ell$ events to test the performance of the method on a known resonance with similar topology. In this test, the peak and width of the relativistic Breit–Wigner function are set to those of the Z boson. The measured Z boson mass was found to be 91.62 ± 0.35 GeV including statistical and systematic uncertainty. The observed uncertainty is in agreement with the expectation of ± 0.34 GeV, as evaluated from simulation. The measured value is in agreement with the world average of 91.1876 ± 0.0021 GeV [48].

As an independent check, the template method [7] is also used to measure m_H . The simulated distributions of the samples generated for m_H values between 110 and 130 GeV are smoothed with a kernel density estimate technique, and then parametrised as a function of m_H by means of a B-spline interpolation to obtain the signal model for any value of m_H . The expected statistical uncertainty of m_H obtained with the per-event method from a

² Four per final state for each of the four BDT categories.

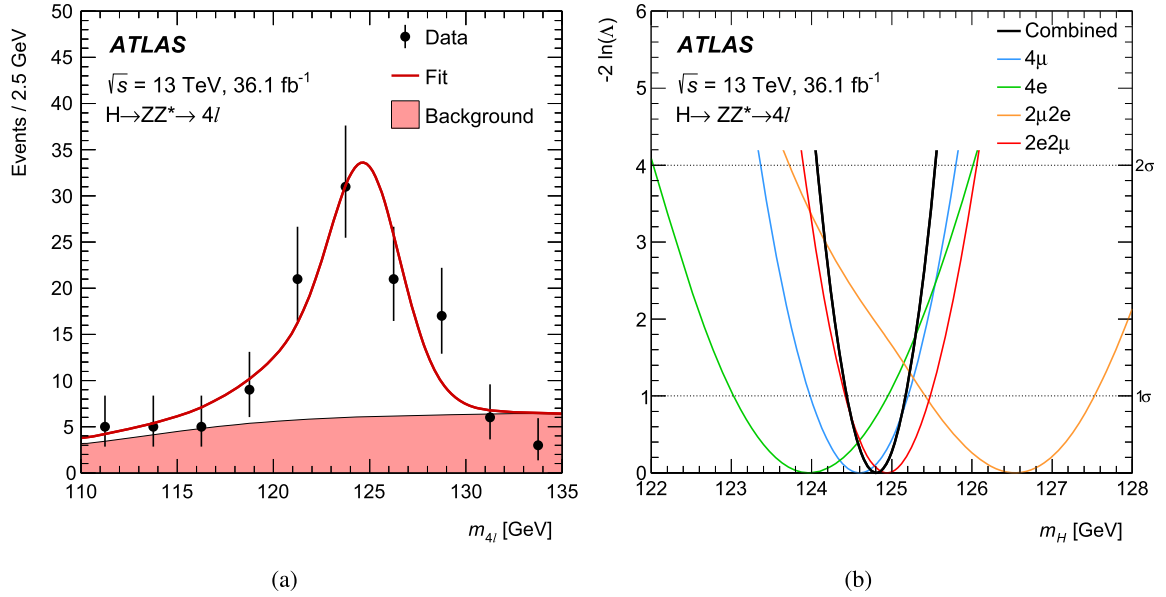


Fig. 1. (a) Invariant mass distribution for the data (points with error bars) shown together with the simultaneous fit result to $H \rightarrow ZZ^* \rightarrow 4\ell$ candidates (continuous line). The background component of the fit is also shown (filled area). The signal probability density function is evaluated per-event and averaged over the observed data. (b) Value of $-2 \ln \Lambda$ as a function of m_H for the combined fit to all $H \rightarrow ZZ^* \rightarrow 4\ell$ categories. The intersection of the $-2 \ln \Lambda$ curve with the horizontal lines labelled 1σ and 2σ provide the 68.3% and 95.5% confidence intervals.

sample equal in size to the experimental data set is, on average, 3% smaller than the statistical uncertainty obtained with the template method. Both methods are found to be unbiased within the statistical uncertainty of the simulated samples used of about 8 MeV on m_H .

7.3. Results

The estimate of m_H for the per-event and template methods is extracted with a simultaneous profile likelihood fit to the sixteen categories. The free parameters of the fit are m_H , the normalisation modifiers of each BDT category, and the nuisance parameters associated with systematic uncertainties. The measured value of m_H from the per-event method is found to be $m_H^{ZZ^*} = 124.79 \pm 0.36$ (stat) ± 0.05 (syst) GeV = 124.79 ± 0.37 GeV.

The total uncertainty is in agreement with the expectation and is dominated by the statistical component. The root-mean-square of the expected uncertainty due to statistical fluctuations in the event yields of each category was estimated to be 40 MeV. The p -value of the uncertainty being as high or higher than the observed value, estimated with pseudo-experiments, is found to be 0.47. The total systematic uncertainty is 50 MeV, the leading sources being the muon momentum scale (40 MeV) and the electron energy scale (26 MeV), with other sources (background modelling and simulation statistics) being smaller than 10 MeV.

For the template method, the total uncertainty is found to be $^{+0.41}_{-0.39}$ GeV, larger by 35 MeV than for the per-event method. The observed difference for the m_H estimates of the two methods is found to be 0.16 GeV, which is compatible with the expected variance estimated with pseudo-experiments and corresponds to a one sided p -value of 0.19. Fig. 1(a) shows the $m_{4\ell}$ distribution of the data together with the result of the fit to the $H \rightarrow ZZ^* \rightarrow 4\ell$ candidates when using the per-event method. The fit is also performed independently for each decay channel, fitting all BDT categories simultaneously; the resulting likelihood profile is compared with the combined fit in Fig. 1(b). The combined measured value of m_H is found to be compatible with the value measured independently for each channel, with the largest deviation being 1.4σ for the $2\mu 2e$ channel and the others being within 1σ .

The Higgs boson mass in the four-lepton channel is also measured by using a profile likelihood ratio to combine the information from the Run 1 analysis [6], where $m_H = 124.51 \pm 0.52$ GeV, and the Run 2 analysis, keeping each individual signal normalisation parameter independent. The systematic uncertainties taken to be correlated between the two runs are the muon momentum and electron energy scales, while all other systematic uncertainties are considered uncorrelated. The combined Run 1 and Run 2 result is $m_H^{ZZ^*} = 124.71 \pm 0.30$ (stat) ± 0.05 (syst) GeV = 124.71 ± 0.30 GeV. The difference between the measured values of m_H in the four-lepton channel in the two runs is $\Delta m_H^{ZZ^*} = 0.28 \pm 0.63$ GeV, with the two results being compatible, with a p -value of 0.84.

8. Mass measurement in the $H \rightarrow \gamma\gamma$ channel

In the diphoton channel, the Higgs boson mass is measured from the position of the narrow resonant peak in the $m_{\gamma\gamma}$ distribution due to the Higgs boson decay to two photons. Such a peak is observed over a large, monotonically decreasing, $m_{\gamma\gamma}$ distribution from continuum background events. The diphoton invariant mass is computed from the measured photon energies and from their directions relative to the diphoton production vertex, chosen among all reconstructed primary vertex candidates using a neural-network algorithm based on track and primary vertex information, as well as the directions of the two photons measured in the calorimeter and inner detector [49].

Events are selected and divided into categories with different mass resolutions and signal-to-background ratios, optimised for the measurement of simplified template cross-sections [30,50] and of production mode signal strengths of the Higgs boson in the diphoton decay channel. The event selection and classification are described in Ref. [24]. A potential reduction of the total expected uncertainty by 4% could have been obtained using the same event categories chosen for the mass measurement with the Run 1 data [7]. Given the small expected improvement, a choice was made to use the same categorisation for the measurement of the mass and of the production mode signal strengths.

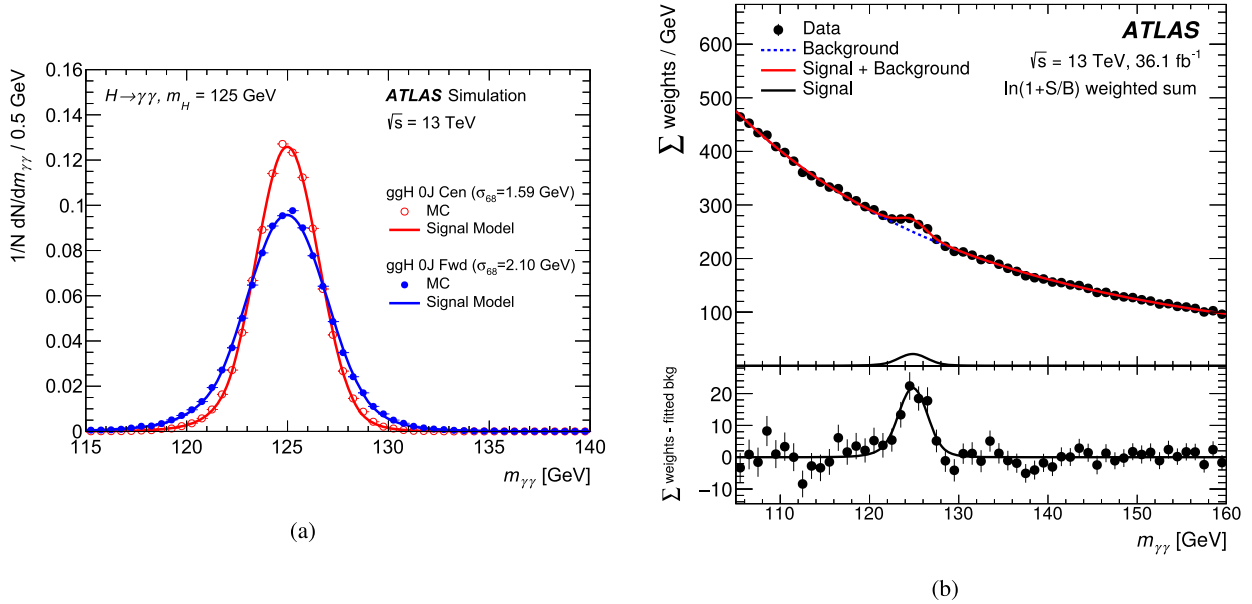


Fig. 2. (a) Invariant mass distributions (circles) of simulated $H \rightarrow \gamma\gamma$ events reconstructed in two categories with one of the best (“ggH 0J Cen”: open circles) and one of the worst (“ggH 0J Fwd”: solid circles) experimental resolutions. The signal model derived from a fit of the simulated events is superimposed (solid lines). (b) Diphoton invariant mass distribution of all selected data events, overlaid with the result of the fit (solid red line). Both for data and for the fit, each category is weighted by a factor $\ln(1+S/B)$, where S and B are the fitted signal and background yields in a $m_{\gamma\gamma}$ interval containing 90% of the expected signal. The dotted line describes the background component of the model. The bottom inset shows the difference between the sum of weights and the background component of the fitted model (dots), compared with the signal model (black line). (For interpretation of the colours in the figure(s), the reader is referred to the web version of this article.)

8.1. Event selection and categorisation

After an initial preselection, described in Ref. [24], requiring the presence of at least two loosely identified photon candidates with $|\eta| < 1.37$ or $1.52 < |\eta| < 2.37$, events are selected if the leading and the subleading photon candidates have $E_T/m_{\gamma\gamma} > 0.35$ and 0.25 respectively, and satisfy the tight identification criteria and isolation criteria based on calorimeter and tracking information. Only events with invariant mass of the leading and subleading photon in the range $105 \text{ GeV} < m_{\gamma\gamma} < 160 \text{ GeV}$ are kept.

The events passing the previous selection are then classified, according to the properties of the two selected photons and of jets, electrons, muons and missing transverse momentum, into 31 mutually exclusive categories [24]. The most populated class, targeting gluon–gluon fusion production without reconstructed jets, is split into two categories of events with very different energy resolution: the first (“ggH 0J Cen”) requires both photons to have $|\eta| < 0.95$, while the second (“ggH 0J Fwd”) retains the remaining events.

8.2. Signal and background models

For each category, the shape of the diphoton invariant mass distribution of the signal is modelled with a double-sided Crystal Ball function [51], i.e. a Gaussian function in the peak region with power-law functions in both tails. The dependence of the parameters on the Higgs boson mass m_H is described by first-order polynomials, whose parameters are fixed by fitting simultaneously all the simulated signal samples generated for different values of m_H .

The quantity σ_{68} , defined as half of the smallest range containing 68% of the expected signal events, is an estimate of the signal $m_{\gamma\gamma}$ resolution and for $m_H = 125 \text{ GeV}$ it ranges between 1.41 GeV and 2.10 GeV depending on the category, while for the inclusive case its value is 1.84 GeV. Fig. 2(a) shows an example of the signal model for a category with one of the best invariant mass resolutions and for a category with one of the worst resolutions.

The expected signal yield is expressed as the product of integrated luminosity, production cross-section, diphoton branching ratio, acceptance and efficiency. The cross-section is parameterised as a function of m_H separately for each production mode. Similarly, the branching ratio is parameterised as a function of m_H . The product of acceptance and efficiency is evaluated separately for each production mode using only the samples with $m_H = 125 \text{ GeV}$. Its dependence on the mass is weak (relative variation below 1% when varying the Higgs boson mass by $\pm 1 \text{ GeV}$) and is thus neglected. The cross-sections are fixed to the SM values multiplied by a signal modifier for each production mode: μ_{ggF} , μ_{VBF} , μ_{VH} and μ_{tH} . The expected yield for $m_H = 125 \text{ GeV}$ varies between about one event in categories sensitive to rare production modes ($t\bar{t}H$, tH) to almost 500 events in the most populated event category (“ggH 0J Fwd”).

The background invariant mass distribution of each category is parameterised with an empirical continuous function of the diphoton system invariant mass value. The parameters of these functions are fitted directly to data. The functional form used to describe the background in each category is chosen among several alternatives according to the three criteria described in Ref. [24]: (i) the fitted signal yield in a test sample representative of the data background, built by combining simulation and control regions in data, must be minimised; (ii) the χ^2 probability for the fit of this background control sample must be larger than a certain threshold; (iii) the quality of the fit to data sidebands must not improve significantly when adding an extra degree of freedom to the model. The models selected by this procedure are exponential or power-law functions with one degree of freedom for the categories with few events, while exponential functions of a second-order polynomial are used for the others.

From the extrapolation of a background-only fit to the sidebands of the $m_{\gamma\gamma}$ distribution in data, excluding events with $121 \text{ GeV} < m_{\gamma\gamma} < 129 \text{ GeV}$, the expected signal-to-background ratio in a $m_{\gamma\gamma}$ window containing 90% of the signal distribution for $m_H = 125 \text{ GeV}$ varies between 2% in the “ggH 0J Fwd” category and 100% in a high-purity, low-yield (about 12 events) category

targeting $H+2\text{jet}$, VBF-like events with low transverse momentum of the $H+2\text{jet}$ system.

8.3. Systematic uncertainties

The main sources of systematic uncertainty in the measured Higgs boson mass in the diphoton channel are the uncertainties in the photon energy scale (PES), the uncertainty arising from the background model, and the uncertainty in the selection of the diphoton production vertex. They are described in detail in Ref. [24].

For each source of uncertainty in the PES described in Section 5, the diphoton invariant mass distribution for each category is re-computed after varying the photon energy by its uncertainty and is then compared with the nominal distribution. The sum in quadrature of the positive or negative shifts of the $m_{\gamma\gamma}$ peak position due to such variations ranges from ± 260 MeV in the “ggH OJ Cen” category to ± 470 MeV in the “jet BSM” category, which requires at least one jet with $p_T > 200$ GeV. All the PES effects are considered as fully correlated across categories.

The uncertainty due to the background modelling is evaluated following the procedure described in Ref. [7]. The expected signal contribution as predicted by the signal model is added to the background control sample. The bias in the estimated Higgs boson mass from a signal-plus-background fit to the test sample relative to the injected mass is considered as a systematic uncertainty due to the background modelling. Its value is around ± 60 MeV for the most relevant categories for the mass measurement. In the other categories it can assume larger values, which are compatible with statistical fluctuations of the background control sample. For this reason this systematic uncertainty is ignored in the poorly populated $t\bar{t}H$ categories, which give a negligible contribution to the mass measurement. This systematic uncertainty is assumed to be uncorrelated between different categories.

The systematic uncertainty related to the selection of the diphoton production vertex is evaluated using $Z \rightarrow ee$ events, as described in Ref. [7]. An expected uncertainty of ± 40 MeV in m_H is used for all the categories and assumed to be fully correlated across different categories.

Systematic uncertainties in the diphoton mass resolution due to uncertainties in the photon energy resolution vary between $\pm 6\%$ (for the “ggH OJ Cen” category) and 11% (for the “jet BSM” category), and are expected to have a negligible impact on the mass measurement.

Systematic uncertainties in the yield and in the migration of events between categories described in Ref. [24] have a negligible impact on the mass measurement.

The uncertainty due to the signal modelling is evaluated similarly to that due to the background modelling. A sample is built using the expected background distribution and the simulated signal events at $m_H = 125$ GeV. The bias in the fitted Higgs boson mass is considered as a systematic uncertainty and is assumed to be correlated between different categories. The relative bias is below 10^{-4} in most of the categories, and at most a few times 10^{-4} in the other categories.

8.4. Results

The Higgs boson mass in the diphoton channel is estimated with a simultaneous binned maximum-likelihood fit to the $m_{\gamma\gamma}$ distributions of the selected event categories. In each category, the distribution is modelled with a sum of the background and signal models. The free parameters of the fit are m_H , the four signal strengths, the number of background events and the parameters

describing the shape of the background invariant mass distribution in each category, and all the nuisance parameters associated with systematic uncertainties. Fig. 2(b) shows the distribution of the data overlaid with the result of the simultaneous fit. All event categories are included. For illustration purposes, events in each category are weighted by a factor $\ln(1 + S/B)$, where S and B are the fitted signal and background yields in a $m_{\gamma\gamma}$ interval containing 90% of the signal.

The measured mass of the Higgs boson in the diphoton channel is $m_H^{\gamma\gamma} = 124.93 \pm 0.21$ (stat) ± 0.34 (syst) GeV = 124.93 ± 0.40 GeV where the first error is the statistical uncertainty while the second is the total systematic uncertainty, dominated by the photon energy scale uncertainty.

Assuming signal strengths as in the SM and the signal model determined from the simulation, the expected statistical uncertainty is 0.25 GeV and the expected total uncertainty is 0.41 GeV, with a root-mean-square, estimated from pseudo-experiments, of about 40 MeV. Compared to the expectation, the slightly larger systematic uncertainty and smaller statistical uncertainty observed in data are due to a lower than expected signal yield in some categories with large expected yield and small photon energy scale uncertainty, and to the fitted resolution in data being a few percent better than in the simulation (but still agreeing with it within one standard deviation).

To check if the measurement is sensitive to the assumption about the splitting of the production modes, the measurement is repeated using one common signal strength for all the processes. A small shift of the measured m_H by 20 MeV is observed. The mass measurement is also performed by allowing the overall signal yield in each analysis category to float independently in the fit. The measured value of m_H changes by less than 30 MeV.

Other checks targeting possible miscalibration due to detector effects for some specific category of photons are performed by partitioning the entire data sample into detector-oriented categories, different from those used for the nominal result, and determining the probability that m_H measured in one of these categories is compatible with the average m_H from the other categories. A first categorisation is based on whether the photons are reconstructed as converted or not, a second is based on the photons' impact points in the calorimeter (either in the barrel region, $|\eta| < 1.37$, or in the endcap region, $|\eta| > 1.52$), and a third is based on the number of interactions per bunch crossing. For each of these categories a new background model, a new signal model and new systematic uncertainty values are computed. For each category the compatibility of its m_H value with the combined m_H value is tested by considering as an additional likelihood parameter the quantity Δ_i equal to the difference between that category's m_H value and the combined value. No value of Δ_i significantly different from zero is found. A similar test is performed to assess the global compatibility of all the different categories with a common value of m_H . In the three categorisations considered the smallest global p -value is 12%. The same procedure is applied to the categories used in the analysis: the smallest p -value computed on single categories is 7% while the global p -value is 94%.

A combination of the Higgs boson mass measured in the diphoton channel by ATLAS in Run 1, 126.02 ± 0.51 GeV [6], and in Run 2 is performed using a profile likelihood ratio. The signal strengths are treated as independent parameters. The systematic uncertainties considered correlated between the two LHC run periods are most of the photon energy scale and resolution uncertainties and those in the pile-up modelling, while all the other systematic uncertainties are considered uncorrelated. The photon energy calibration uncertainties that are treated as uncorrelated between the two LHC data-taking periods are a few uncertainties included only in the Run 2 measurement, the uncertainty

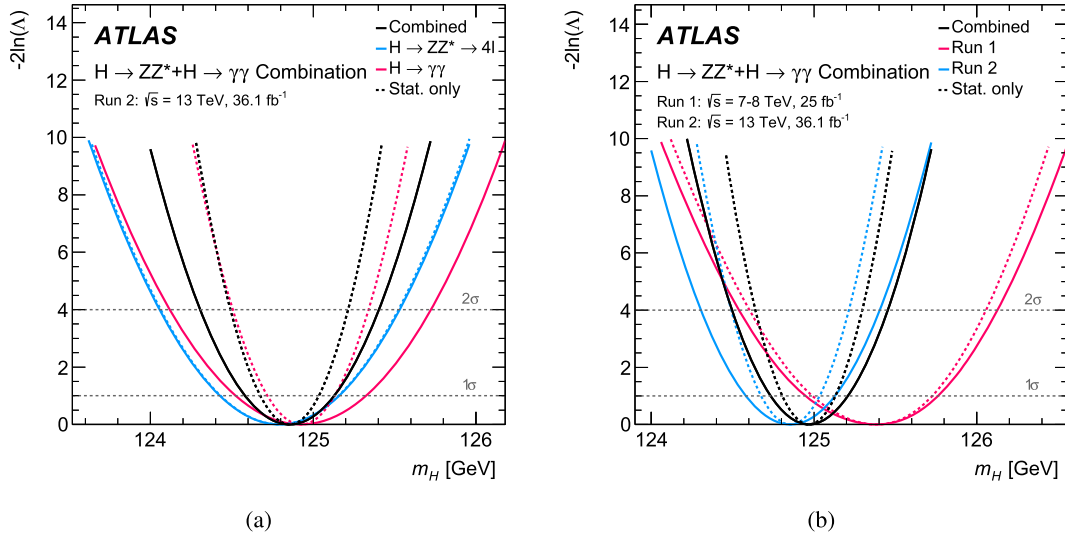


Fig. 3. The value of $-2\ln\Delta$ as a function of m_H for (a) $H \rightarrow \gamma\gamma$, $H \rightarrow ZZ^* \rightarrow 4\ell$ channels and their combination (red, blue and black, respectively) using Run 2 data only and for (b) Run 1, Run 2 and their combination (red, blue and black, respectively). The dashed lines show the mass measurement uncertainties assuming statistical uncertainties only.

in the photon energy leakage outside the reconstructed cluster, whose measurement is limited by the statistical accuracy of $Z \rightarrow \ell\ell\gamma$, and the uncertainty in the electromagnetic calorimeter response non-linearity, which is estimated with different procedures in the two LHC run periods. The result is $m_H^{\gamma\gamma} = 125.32 \pm 0.19$ (stat) ± 0.29 (syst) GeV = 125.32 ± 0.35 GeV. The difference between the measured values of m_H in the diphoton channel in the two LHC run periods is $\Delta m_H^{\gamma\gamma} = 1.09 \pm 0.46$ (stat) ± 0.34 (syst) GeV = 1.09 ± 0.57 GeV. The probability that the two results are compatible is 5.1%.

9. Combined mass measurement

The Higgs boson mass is measured by combining information from both the $H \rightarrow ZZ^* \rightarrow 4\ell$ and $H \rightarrow \gamma\gamma$ channels. The correlations between the systematic uncertainties in the two channels are accounted for in the profile likelihood function. The main sources of correlated systematic uncertainty include the calibrations of electrons and photons, the pile-up modelling, and the luminosity. Signal yield normalisations are treated as independent free parameters in the fit to minimise model-dependent assumptions in the measurement of the Higgs boson mass.

The combined value of the mass measured using Run 2 data is $m_H = 124.86 \pm 0.27$ GeV. Assuming statistical uncertainties only, the uncertainty in the combined value is ± 0.18 GeV. The corresponding profile likelihood, for the two channels and for their combination, is shown in Fig. 3(a). This result is in good agreement with the ATLAS+CMS Run 1 measurement [6], $m_H = 125.09 \pm 0.24$ GeV.

The combined mass measurement from the ATLAS Run 1 ($m_H = 125.36 \pm 0.41$ GeV) and Run 2 results is $m_H = 124.97 \pm 0.24$ GeV. Assuming statistical uncertainties only, the measurement uncertainty amounts to 0.16 GeV. Fig. 3(b) shows the value of $-2\ln\Delta$ as a function of m_H for the two channels combined, separately for the ATLAS Run 1 and Run 2 data sets, as well as for their combination.

The contributions of the main sources of systematic uncertainty to the combined mass measurement, using both ATLAS Run 1 and Run 2 data, are summarised in Table 1. The impact of each source of systematic uncertainty is evaluated starting from the contribution of each individual nuisance parameter to the total uncertainty. This contribution is defined as the mass shift δm_H observed when

Table 1

Main sources of systematic uncertainty in the Higgs boson mass m_H measured with the 4ℓ and $\gamma\gamma$ final states using Run 1 and Run 2 data. The sum in quadrature of the individual contributions is not expected to reproduce the total systematic uncertainty due to the different methodologies employed to derive them.

Source	Systematic uncertainty in m_H [MeV]
EM calorimeter response linearity	60
Non-ID material	55
EM calorimeter layer intercalibration	55
$Z \rightarrow ee$ calibration	45
ID material	45
Lateral shower shape	40
Muon momentum scale	20
Conversion reconstruction	20
$H \rightarrow \gamma\gamma$ background modelling	20
$H \rightarrow \gamma\gamma$ vertex reconstruction	15
e/γ energy resolution	15
All other systematic uncertainties	10

re-evaluating the profile likelihood ratio after fixing the nuisance parameter in question to its best-fit value increased or decreased by one standard deviation, while all remainder nuisance parameters remain free to float. The sum in quadrature of groups of nuisance parameter variations gives the impact of each category of systematic uncertainties. The nuisance parameter values from the unconditional maximum-likelihood fit are consistent with the pre-fit values within one standard deviation.

The probability that the m_H results from the four measurements (in the 4ℓ and $\gamma\gamma$ final states, using Run 1 or Run 2 ATLAS data) are compatible is 12.3%. Due to the impact of the correlated systematic uncertainties, the correlation between m_H in the $H \rightarrow \gamma\gamma$ channel over the two runs is 23%. The residual correlation between $H \rightarrow ZZ^* \rightarrow 4\ell$ and $H \rightarrow \gamma\gamma$ is typically 1%. The results from each of the four individual measurements, as well as various combinations, along with the LHC Run 1 result, are summarised in Fig. 4.

The combination of the four ATLAS measurements using the BLUE approach as an alternative method, assuming two uncorrelated channels,³ is found to be $m_H = 124.97 \pm 0.23$ GeV =

³ The combination of the two LHC run periods for each channel was used as input.

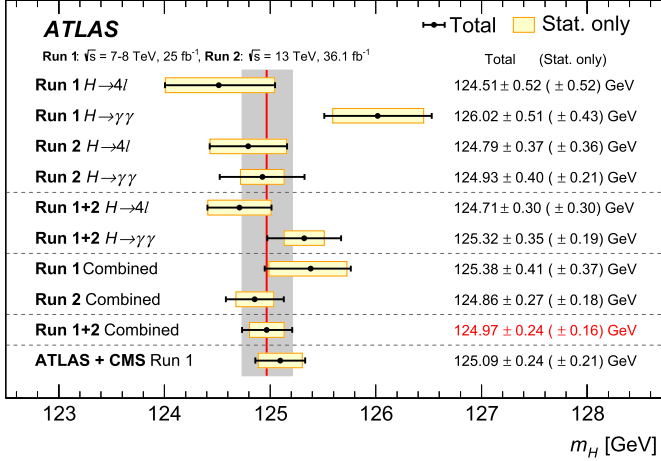


Fig. 4. Summary of the Higgs boson mass measurements from the individual and combined analyses performed here, compared with the combined Run 1 measurement by ATLAS and CMS [6]. The statistical-only (horizontal yellow-shaded bands) and total (black error bars) uncertainties are indicated. The (red) vertical line and corresponding (grey) shaded column indicate the central value and the total uncertainty of the combined ATLAS Run 1 + 2 measurement, respectively.

124.97 ± 0.19 (stat) ± 0.13 (syst) GeV. The splitting of the errors takes into account the relative weight of the two channels in the combined measurement.

10. Conclusion

The mass of the Higgs boson has been measured from a combined fit to the invariant mass spectra of the decay channels $H \rightarrow ZZ^* \rightarrow 4l$ and $H \rightarrow \gamma\gamma$. The results are obtained from a Run 2 pp collision data sample recorded by the ATLAS experiment at the CERN Large Hadron Collider at a centre-of-mass energy of 13 TeV, corresponding to an integrated luminosity of 36.1 fb^{-1} . The measurements are based on the latest calibrations of muons, electrons, and photons, and on improvements to the analysis techniques used to obtain the previous results from ATLAS Run 1 data.

The measured values of the Higgs boson mass for the $H \rightarrow ZZ^* \rightarrow 4l$ and $H \rightarrow \gamma\gamma$ channels are

$$m_H = 124.79 \pm 0.37 \text{ GeV},$$

$$m_H = 124.93 \pm 0.40 \text{ GeV}.$$

From the combination of these two channels, the mass is measured to be

$$m_H = 124.86 \pm 0.27 \text{ GeV}.$$

This result is in good agreement with the average of the ATLAS and CMS Run 1 measurements. The combination of the ATLAS Run 1 and Run 2 measurements yields

$$m_H = 124.97 \pm 0.24 \text{ GeV}.$$

Acknowledgements

We thank CERN for the very successful operation of the LHC, as well as the support staff from our institutions without whom ATLAS could not be operated efficiently.

We acknowledge the support of ANPCyT, Argentina; YerPhI, Armenia; ARC, Australia; BMWFW and FWF, Austria; ANAS, Azerbaijan; SSTC, Belarus; CNPq and FAPESP, Brazil; NSERC, NRC and CFI, Canada; CERN; CONICYT, Chile; CAS, MOST and NSFC, China;

COLCIENCIAS, Colombia; MSMT CR, MPO CR and VSC CR, Czech Republic; DNRF and DNSRC, Denmark; IN2P3-CNRS, CEA-DRF/IRFU, France; SRNSFG, Georgia; BMBF, HGF, and MPG, Germany; GSRT, Greece; RGC, Hong Kong SAR, China; ISF, I-CORE and Benoziyo Center, Israel; INFN, Italy; MEXT and JSPS, Japan; CNRST, Morocco; NWO, Netherlands; RCN, Norway; MNiSW and NCN, Poland; FCT, Portugal; MNE/IFA, Romania; MES of Russia and NRC KI, Russian Federation; JINR; MESTD, Serbia; MSSR, Slovakia; ARRS and MIZŠ, Slovenia; DST/NRF, South Africa; MINECO, Spain; SRC and Wallenberg Foundation, Sweden; SERI, SNSF and Cantons of Bern and Geneva, Switzerland; MOST, Taiwan; TAEK, Turkey; STFC, United Kingdom; DOE and NSF, United States of America. In addition, individual groups and members have received support from BCKDF, the Canada Council, Canarie, CRC, Compute Canada, FQRNT, and the Ontario Innovation Trust, Canada; EPLANET, ERC, ERDF, FP7, Horizon 2020 and Marie Skłodowska-Curie Actions, European Union; Investissements d'Avenir Labex and Idex, ANR, Région Auvergne and Fondation Partager le Savoir, France; DFG and AvH Foundation, Germany; Herakleitos, Thales and Aristeia programmes co-financed by EU-ESF and the Greek NSRF; BSF, GIF and Minerva, Israel; BRF, Norway; CERCA Programme Generalitat de Catalunya, Generalitat Valenciana, Spain; the Royal Society and Leverhulme Trust, United Kingdom.

The crucial computing support from all WLCG partners is acknowledged gratefully, in particular from CERN, the ATLAS Tier-1 facilities at TRIUMF (Canada), NDGF (Denmark, Norway, Sweden), CC-IN2P3 (France), KIT/GridKA (Germany), INFN-CNAF (Italy), NL-T1 (Netherlands), PIC (Spain), ASGC (Taiwan), RAL (UK) and BNL (USA), the Tier-2 facilities worldwide and large non-WLCG resource providers. Major contributors of computing resources are listed in Ref. [52].

References

- [1] ATLAS Collaboration, Observation of a new particle in the search for the Standard Model Higgs boson with the ATLAS detector at the LHC, *Phys. Lett. B* 716 (2012) 1, arXiv:1207.7214 [hep-ex].
- [2] CMS Collaboration, Observation of a new boson at a mass of 125 GeV with the CMS experiment at the LHC, *Phys. Lett. B* 716 (2012) 30, arXiv:1207.7235 [hep-ex].
- [3] F. Englert, R. Brout, Broken symmetry and the mass of gauge vector mesons, *Phys. Rev. Lett.* 13 (1964) 321.
- [4] P.W. Higgs, Broken symmetries and the masses of gauge bosons, *Phys. Rev. Lett.* 13 (1964) 508.
- [5] G. Guralnik, C. Hagen, T. Kibble, Global conservation laws and massless particles, *Phys. Rev. Lett.* 13 (1964) 585.
- [6] ATLAS, CMS Collaborations, Combined measurement of the Higgs boson mass in pp collisions at $\sqrt{s} = 7$ and 8 TeV with the ATLAS and CMS experiments, *Phys. Rev. Lett.* 114 (2015) 191803, arXiv:1503.07589 [hep-ex].
- [7] ATLAS Collaboration, Measurement of the Higgs boson mass from the $H \rightarrow \gamma\gamma$ and $H \rightarrow ZZ^* \rightarrow 4l$ channels in pp collisions at center-of-mass energies of 7 and 8 TeV with the ATLAS detector, *Phys. Rev. D* 90 (2014) 052004, arXiv:1406.3827 [hep-ex].
- [8] CMS Collaboration, Precise determination of the mass of the Higgs boson and tests of compatibility of its couplings with the standard model predictions using proton collisions at 7 and 8 TeV, *Eur. Phys. J. C* 75 (2015) 212, arXiv:1412.8662 [hep-ex].
- [9] CMS Collaboration, Measurements of properties of the Higgs boson decaying into the four-lepton final state in pp collisions at $\sqrt{s} = 13$ TeV, *J. High Energy Phys.* 11 (2017) 047, arXiv:1706.09936 [hep-ex].
- [10] ATLAS Collaboration, The ATLAS experiment at the CERN Large Hadron Collider, *J. Instrum.* 3 (2008) S08003.
- [11] ATLAS Collaboration, Measurement of inclusive and differential cross sections in the $H \rightarrow ZZ^* \rightarrow 4l$ decay channel in pp collisions at $\sqrt{s} = 13$ TeV with the ATLAS detector, *J. High Energy Phys.* 10 (2017) 132, arXiv:1708.02810 [hep-ex].
- [12] K. Hamilton, P. Nason, E. Re, G. Zanderighi, NNLOPS simulation of Higgs boson production, *J. High Energy Phys.* 10 (2013) 222, arXiv:1309.0017 [hep-ph].
- [13] J. Butterworth, et al., PDF4LHC recommendations for LHC Run II, *J. Phys. G* 43 (2016) 023001, arXiv:1510.03865 [hep-ph].
- [14] S. Alioli, P. Nason, C. Oleari, E. Re, NLO Higgs boson production via gluon fusion matched with shower in POWHEG, *J. High Energy Phys.* 04 (2009) 002, arXiv:0812.0578 [hep-ph].

- [15] T. Sjöstrand, S. Mrenna, P.Z. Skands, A brief introduction to PYTHIA 8.1, *Comput. Phys. Commun.* 178 (2008) 852, arXiv:0710.3820 [hep-ph].
- [16] D.J. Lange, The EvtGen particle decay simulation package, *Nucl. Instrum. Methods A* 462 (2001) 152.
- [17] H.-L. Lai, et al., New parton distributions for collider physics, *Phys. Rev. D* 82 (2010) 074024, arXiv:1007.2241 [hep-ph].
- [18] J. Pumplin, et al., New generation of parton distributions with uncertainties from global QCD analysis, *J. High Energy Phys.* 07 (2002) 012, arXiv:hep-ph/0201195 [hep-ph].
- [19] ATLAS Collaboration, Measurement of the Z/γ^* boson transverse momentum distribution in pp collisions at $\sqrt{s} = 7$ TeV with the ATLAS detector, *J. High Energy Phys.* 09 (2014) 145, arXiv:1406.3660 [hep-ex].
- [20] F. Cascioli, et al., ZZ production at hadron colliders in NNLO QCD, *Phys. Lett. B* 735 (2014) 311, arXiv:1405.2219 [hep-ph].
- [21] M. Grazzini, S. Kallweit, D. Rathlev, ZZ production at the LHC: fiducial cross sections and distributions in NNLO QCD, *Phys. Lett. B* 750 (2015) 407, arXiv:1507.06257 [hep-ph].
- [22] B. Biedermann, A. Denner, S. Dittmaier, L. Hofer, B. Jäger, Electroweak corrections to $pp \rightarrow \mu^+ \mu^- e^+ e^- + X$ at the LHC: a Higgs boson background study, *Phys. Rev. Lett.* 116 (2016) 161803, arXiv:1601.07787 [hep-ph].
- [23] B. Biedermann, A. Denner, S. Dittmaier, L. Hofer, B. Jäger, Next-to-leading-order electroweak corrections to the production of four charged leptons at the LHC, *J. High Energy Phys.* 01 (2017) 033, arXiv:1611.05338 [hep-ph].
- [24] ATLAS Collaboration, Measurements of Higgs boson properties in the diphoton decay channel with 36 fb^{-1} of pp collision data at $\sqrt{s} = 13$ TeV with the ATLAS detector, arXiv:1802.04146 [hep-ex], 2018.
- [25] ATLAS Collaboration, The ATLAS simulation infrastructure, *Eur. Phys. J. C* 70 (2010) 823, arXiv:1005.4568 [physics.ins-det].
- [26] S. Agostinelli, et al., GEANT4 – a simulation toolkit, *Nucl. Instrum. Methods A* 506 (2003) 250.
- [27] LHC Higgs Cross Section Working Group, S. Dittmaier, C. Mariotti, G. Passarino, R. Tanaka (Eds.), *Handbook of LHC Higgs Cross Sections: 1. Inclusive Observables*, CERN, Geneva, 2011, CERN-2011-002, arXiv:1101.0593 [hep-ph].
- [28] LHC Higgs Cross Section Working Group, S. Dittmaier, C. Mariotti, G. Passarino, R. Tanaka (Eds.), *Handbook of LHC Higgs Cross Sections: 2. Differential Distributions*, CERN, Geneva, 2012, CERN-2012-002, arXiv:1201.3084 [hep-ph].
- [29] LHC Higgs Cross Section Working Group, S. Heinemeyer, C. Mariotti, G. Passarino, R. Tanaka (Eds.), *Handbook of LHC Higgs Cross Sections: 3. Higgs Properties*, CERN, Geneva, 2013, CERN-2013-004, arXiv:1307.1347 [hep-ph].
- [30] LHC Higgs Cross Section Working Group, D. de Florian, C. Grojean, F. Maltoni, C. Mariotti, A. Nikitenko, M. Pieri, P. Savard, M. Schumacher, R. Tanaka (Eds.), *Handbook of LHC Higgs Cross Sections: 4. Deciphering the Nature of the Higgs Sector*, CERN, Geneva, 2017, CERN-2017-002, arXiv:1610.07922 [hep-ph].
- [31] ATLAS Collaboration, Early inner detector tracking performance in the 2015 data at $\sqrt{s} = 13$ TeV, ATL-PHYS-PUB-2015-051, URL: <https://cds.cern.ch/record/2110140>, 2015.
- [32] ATLAS Collaboration, Study of alignment-related systematic effects on the ATLAS Inner Detector track reconstruction, ATLAS-CONF-2012-141, URL: <https://cds.cern.ch/record/1483518>, 2012.
- [33] ATLAS Collaboration, Muon reconstruction performance of the ATLAS detector in proton–proton collision data at $\sqrt{s} = 13$ TeV, *Eur. Phys. J. C* 76 (2016) 292, arXiv:1603.05598 [hep-ex].
- [34] ATLAS Collaboration, Topological cell clustering in the ATLAS calorimeters and its performance in LHC Run 1, *Eur. Phys. J. C* 77 (2017) 490, arXiv:1603.02934 [hep-ex].
- [35] ATLAS Collaboration, Measurement of the photon identification efficiencies with the ATLAS detector using LHC Run-1 data, *Eur. Phys. J. C* 76 (2016) 666, arXiv:1606.01813 [hep-ex].
- [36] ATLAS Collaboration, Electron and photon energy calibration with the ATLAS detector using LHC Run 1 data, *Eur. Phys. J. C* 74 (2014) 3071, arXiv:1407.5063 [hep-ex].
- [37] ATLAS Collaboration, Electron and photon energy calibration with the ATLAS detector using data collected in 2015 at $\sqrt{s} = 13$ TeV, ATL-PHYS-PUB-2016-015, URL: <https://cds.cern.ch/record/2203514>, 2016.
- [38] ATLAS Collaboration, Electron efficiency measurements with the ATLAS detector using 2012 LHC proton–proton collision data, *Eur. Phys. J. C* 77 (2017) 195, arXiv:1612.01456 [hep-ex].
- [39] ATLAS Collaboration, Combined search for the Standard Model Higgs boson in pp collisions at $\sqrt{s} = 7$ TeV with the ATLAS detector, *Phys. Rev. D* 86 (2012) 032003, arXiv:1207.0319 [hep-ex].
- [40] G. Cowan, K. Cranmer, E. Gross, O. Vitells, Asymptotic formulae for likelihood-based tests of new physics, *Eur. Phys. J. C* 71 (2011) 1554, arXiv:1007.1727.
- [41] R. Nisius, On the combination of correlated estimates of a physics observable, *Eur. Phys. J. C* (ISSN 1434-6052) 74 (2014) 3004, <https://doi.org/10.1140/epjc/s10052-014-3004-2>.
- [42] L. Lyons, D. Gibaut, P. Clifford, How to combine correlated estimates of a single physical quantity, *Nucl. Instrum. Methods A* 270 (1988) 110.
- [43] A. Valassi, Combining correlated measurements of several different physical quantities, *Nucl. Instrum. Methods A* 500 (2003) 391.
- [44] M. Aaboud, et al., Measurement of the Higgs boson coupling properties in the $H \rightarrow ZZ^* \rightarrow 4\ell$ decay channel at $\sqrt{s} = 13$ TeV with the ATLAS detector, *J. High Energy Phys.* 03 (2018) 095, arXiv:1712.02304 [hep-ex].
- [45] ATLAS Collaboration, Measurements of Higgs boson production and couplings in the four-lepton channel in pp collisions at center-of-mass energies of 7 and 8 TeV with the ATLAS detector, *Phys. Rev. D* 91 (2015) 012006, arXiv:1408.5191 [hep-ex].
- [46] R. Frühwirth, Track fitting with non-Gaussian noise, *Comput. Phys. Commun.* 100 (1997) 1.
- [47] ATLAS Collaboration, Improved electron reconstruction in ATLAS using the Gaussian Sum Filter-based model for bremsstrahlung, ATLAS-CONF-2012-047, URL: <https://cds.cern.ch/record/1449796>, 2012.
- [48] M. Tanabashi, et al., Particle Data Group, Review of particle physics, *Phys. Rev. D* 98 (2018) 010001.
- [49] ATLAS Collaboration, Measurement of Higgs boson production in the diphoton decay channel in pp collisions at center-of-mass energies of 7 and 8 TeV with the ATLAS detector, *Phys. Rev. D* 90 (2014) 112015, arXiv:1408.7084 [hep-ex].
- [50] J.R. Andersen, et al., Les Houches 2015: physics at TeV colliders standard model working group report, arXiv:1605.04692 [hep-ph].
- [51] ATLAS Collaboration, Search for resonances in diphoton events at $\sqrt{s} = 13$ TeV with the ATLAS detector, *J. High Energy Phys.* 09 (2016) 001, arXiv:1606.03833 [hep-ex].
- [52] ATLAS Collaboration, ATLAS computing acknowledgements, ATL-GEN-PUB-2016-002, URL: <https://cds.cern.ch/record/2202407>.

The ATLAS Collaboration

M. Aaboud^{34d}, G. Aad⁹⁹, B. Abbott¹²⁴, O. Abdinov^{13,*}, B. Abeloos¹²⁸, S.H. Abidi¹⁶⁵, O.S. AbouZeid¹⁴³, N.L. Abraham¹⁵³, H. Abramowicz¹⁵⁹, H. Abreu¹⁵⁸, Y. Abulaiti⁶, B.S. Acharya^{64a,64b,o}, S. Adachi¹⁶¹, L. Adamczyk^{81a}, J. Adelman¹¹⁹, M. Adersberger¹¹², T. Adye¹⁴¹, A.A. Affolder¹⁴³, Y. Afik¹⁵⁸, C. Agheorghiesei^{27c}, J.A. Aguilar-Saavedra^{136f,136a}, F. Ahmadov^{77,ag}, G. Aielli^{71a,71b}, S. Akatsuka⁸³, T.P.A. Åkesson⁹⁴, E. Akilli⁵², A.V. Akimov¹⁰⁸, G.L. Alberghi^{23b,23a}, J. Albert¹⁷⁴, P. Albicocco⁴⁹, M.J. Alconada Verzini⁸⁶, S. Alderweireldt¹¹⁷, M. Aleksa³⁵, I.N. Aleksandrov⁷⁷, C. Alexa^{27b}, G. Alexander¹⁵⁹, T. Alexopoulos¹⁰, M. Alhroob¹²⁴, B. Ali¹³⁸, G. Alimonti^{66a}, J. Alison³⁶, S.P. Alkire¹⁴⁵, C. Allaire¹²⁸, B.M.M. Allbrooke¹⁵³, B.W. Allen¹²⁷, P.P. Allport²¹, A. Aloisio^{67a,67b}, A. Alonso³⁹, F. Alonso⁸⁶, C. Alpigiani¹⁴⁵, A.A. Alshehri⁵⁵, M.I. Alstady⁹⁹, B. Alvarez Gonzalez³⁵, D. Álvarez Piqueras¹⁷², M.G. Alviggi^{67a,67b}, B.T. Amadio¹⁸, Y. Amaral Coutinho^{78b}, L. Ambroz¹³¹, C. Amelung²⁶, D. Amidei¹⁰³, S.P. Amor Dos Santos^{136a,136c}, S. Amoroso³⁵, C.S. Amrouche⁵², C. Anastopoulos¹⁴⁶, L.S. Ancu⁵², N. Andari²¹, T. Andeen¹¹, C.F. Anders^{59b}, J.K. Anders²⁰, K.J. Anderson³⁶, A. Andreazza^{66a,66b}, V. Andrei^{59a}, S. Angelidakis³⁷, I. Angelozzi¹¹⁸, A. Angerami³⁸, A.V. Anisenkov^{120b,120a}, A. Annovi^{69a}, C. Antel^{59a}, M.T. Anthony¹⁴⁶, M. Antonelli⁴⁹, D.J.A. Antrim¹⁶⁹, F. Anulli^{70a}, M. Aoki⁷⁹, L. Aperio Bella³⁵, G. Arabidze¹⁰⁴, Y. Arai⁷⁹, J.P. Araque^{136a}, V. Araujo Ferraz^{78b}, R. Araujo Pereira^{78b}, A.T.H. Arce⁴⁷, R.E. Ardell⁹¹, F.A. Arduh⁸⁶, J-F. Arguin¹⁰⁷, S. Argyropoulos⁷⁵,

A.J. Armbruster³⁵, L.J. Armitage⁹⁰, O. Arnaez¹⁶⁵, H. Arnold¹¹⁸, M. Arratia³¹, O. Arslan²⁴,
 A. Artamonov^{109,*}, G. Artoni¹³¹, S. Artz⁹⁷, S. Asai¹⁶¹, N. Asbah⁴⁴, A. Ashkenazi¹⁵⁹,
 E.M. Asimakopoulou¹⁷⁰, L. Asquith¹⁵³, K. Assamagan²⁹, R. Astalos^{28a}, R.J. Atkin^{32a}, M. Atkinson¹⁷¹,
 N.B. Atlay¹⁴⁸, K. Augsten¹³⁸, G. Avolio³⁵, R. Avramidou^{58a}, B. Axen¹⁸, M.K. Ayoub^{15a}, G. Azuelos^{107,au},
 A.E. Baas^{59a}, M.J. Baca²¹, H. Bachacou¹⁴², K. Bachas^{65a,65b}, M. Backes¹³¹, P. Bagnaia^{70a,70b},
 M. Bahmani⁸², H. Bahrasemani¹⁴⁹, A.J. Bailey¹⁷², J.T. Baines¹⁴¹, M. Bajic³⁹, O.K. Baker¹⁸¹, P.J. Bakker¹¹⁸,
 D. Bakshi Gupta⁹³, E.M. Baldin^{120b,120a}, P. Balek¹⁷⁸, F. Balli¹⁴², W.K. Balunas¹³³, E. Banas⁸²,
 A. Bandyopadhyay²⁴, S. Banerjee^{179,k}, A.A.E. Bannoura¹⁸⁰, L. Barak¹⁵⁹, W.M. Barbe³⁷, E.L. Barberio¹⁰²,
 D. Barberis^{53b,53a}, M. Barbero⁹⁹, T. Barillari¹¹³, M-S. Barisits³⁵, J. Barkeloo¹²⁷, T. Barklow¹⁵⁰,
 N. Barlow³¹, R. Barnea¹⁵⁸, S.L. Barnes^{58c}, B.M. Barnett¹⁴¹, R.M. Barnett¹⁸, Z. Barnovska-Blenessy^{58a},
 A. Baroncelli^{72a}, G. Barone²⁶, A.J. Barr¹³¹, L. Barranco Navarro¹⁷², F. Barreiro⁹⁶,
 J. Barreiro Guimarães da Costa^{15a}, R. Bartoldus¹⁵⁰, A.E. Barton⁸⁷, P. Bartos^{28a}, A. Basalae¹³⁴,
 A. Bassalat¹²⁸, R.L. Bates⁵⁵, S.J. Batista¹⁶⁵, S. Batlamous^{34e}, J.R. Batley³¹, M. Battaglia¹⁴³,
 M. Bause^{70a,70b}, F. Bauer¹⁴², K.T. Bauer¹⁶⁹, H.S. Bawa^{150,m}, J.B. Beacham¹²², M.D. Beattie⁸⁷, T. Beau¹³²,
 P.H. Beauchemin¹⁶⁸, P. Bechtel²⁴, H.C. Beck⁵¹, H.P. Beck^{20,r}, K. Becker⁵⁰, M. Becker⁹⁷, C. Becot¹²¹,
 A. Beddall^{12d}, A.J. Beddall^{12a}, V.A. Bednyakov⁷⁷, M. Bedognetti¹¹⁸, C.P. Bee¹⁵², T.A. Beermann³⁵,
 M. Begalli^{78b}, M. Begel²⁹, A. Behera¹⁵², J.K. Behr⁴⁴, A.S. Bell⁹², G. Bella¹⁵⁹, L. Bellagamba^{23b},
 A. Bellerive³³, M. Bellomo¹⁵⁸, K. Belotskiy¹¹⁰, N.L. Belyaev¹¹⁰, O. Benary^{159,*}, D. Bencheikroun^{34a},
 M. Bender¹¹², N. Benekos¹⁰, Y. Benhammou¹⁵⁹, E. Benhar Noccioli¹⁸¹, J. Benitez⁷⁵, D.P. Benjamin⁴⁷,
 M. Benoit⁵², J.R. Bensinger²⁶, S. Bentvelsen¹¹⁸, L. Beresford¹³¹, M. Beretta⁴⁹, D. Berge⁴⁴,
 E. Bergeaas Kuutmann¹⁷⁰, N. Berger⁵, L.J. Bergsten²⁶, J. Beringer¹⁸, S. Berlendis⁵⁶, N.R. Bernard¹⁰⁰,
 G. Bernardi¹³², C. Bernius¹⁵⁰, F.U. Bernlochner²⁴, T. Berry⁹¹, P. Berta⁹⁷, C. Bertella^{15a}, G. Bertoli^{43a,43b},
 I.A. Bertram⁸⁷, C. Bertsche⁴⁴, G.J. Besjes³⁹, O. Bessidskaia Bylund^{43a,43b}, M. Bessner⁴⁴, N. Besson¹⁴²,
 A. Bethani⁹⁸, S. Bethke¹¹³, A. Betti²⁴, A.J. Bevan⁹⁰, J. Beyer¹¹³, R.M.B. Bianchi¹³⁵, O. Biebel¹¹²,
 D. Biedermann¹⁹, R. Bielski⁹⁸, K. Bierwagen⁹⁷, N.V. Biesuz^{69a,69b}, M. Biglietti^{72a}, T.R.V. Billoud¹⁰⁷,
 M. Bindi⁵¹, A. Bingul^{12d}, C. Bini^{70a,70b}, S. Biondi^{23b,23a}, T. Bisanz⁵¹, J.P. Biswal¹⁵⁹, C. Bittrich⁴⁶,
 D.M. Bjergaard⁴⁷, J.E. Black¹⁵⁰, K.M. Black²⁵, R.E. Blair⁶, T. Blazek^{28a}, I. Bloch⁴⁴, C. Blocker²⁶, A. Blue⁵⁵,
 U. Blumenschein⁹⁰, Dr. Blunier^{144a}, G.J. Bobbink¹¹⁸, V.S. Bobrovnikov^{120b,120a}, S.S. Bocchetta⁹⁴,
 A. Bocci⁴⁷, C. Bock¹¹², D. Boerner¹⁸⁰, D. Bogavac¹¹², A.G. Bogdanchikov^{120b,120a}, C. Boehm^{43a},
 V. Boisvert⁹¹, P. Bokan^{170,y}, T. Bold^{81a}, A.S. Boldyrev¹¹¹, A.E. Bolz^{59b}, M. Bomben¹³², M. Bona⁹⁰,
 J.S. Bonilla¹²⁷, M. Boonekamp¹⁴², A. Borisov¹⁴⁰, G. Borissov⁸⁷, J. Bortfeldt³⁵, D. Bortoletto¹³¹,
 V. Bortolotto^{71a,61b,61c,71b}, D. Boscherini^{23b}, M. Bosman¹⁴, J.D. Bossio Sola³⁰, J. Boudreau¹³⁵,
 E.V. Bouhova-Thacker⁸⁷, D. Boumediene³⁷, C. Bourdarios¹²⁸, S.K. Boutle⁵⁵, A. Boveia¹²², J. Boyd³⁵,
 I.R. Boyko⁷⁷, A.J. Bozson⁹¹, J. Bracinik²¹, N. Brahimi⁹⁹, A. Brandt⁸, G. Brandt¹⁸⁰, O. Brandt^{59a},
 F. Braren⁴⁴, U. Bratzler¹⁶², B. Brau¹⁰⁰, J.E. Brau¹²⁷, W.D. Breaden Madden⁵⁵, K. Brendlinger⁴⁴,
 A.J. Brennan¹⁰², L. Brenner⁴⁴, R. Brenner¹⁷⁰, S. Bressler¹⁷⁸, B. Brickwedde⁹⁷, D.L. Briglin²¹,
 T.M. Bristow⁴⁸, D. Britton⁵⁵, D. Britzger^{59b}, I. Brock²⁴, R. Brock¹⁰⁴, G. Brooijmans³⁸, T. Brooks⁹¹,
 W.K. Brooks^{144b}, E. Brost¹¹⁹, J.H. Broughton²¹, P.A. Bruckman de Renstrom⁸², D. Bruncko^{28b},
 A. Bruni^{23b}, G. Bruni^{23b}, L.S. Bruni¹¹⁸, S. Bruno^{71a,71b}, B.H. Brunt³¹, M. Bruschi^{23b}, N. Bruscino¹³⁵,
 P. Bryant³⁶, L. Bryngemark⁴⁴, T. Buanes¹⁷, Q. Buat³⁵, P. Buchholz¹⁴⁸, A.G. Buckley⁵⁵, I.A. Budagov⁷⁷,
 F. Buehrer⁵⁰, M.K. Bugge¹³⁰, O. Bulekov¹¹⁰, D. Bullock⁸, T.J. Burch¹¹⁹, S. Burdin⁸⁸, C.D. Burgard¹¹⁸,
 A.M. Burger⁵, B. Burghgrave¹¹⁹, K. Burka⁸², S. Burke¹⁴¹, I. Burmeister⁴⁵, J.T.P. Burr¹³¹, D. Büscher⁵⁰,
 V. Büscher⁹⁷, E. Buschmann⁵¹, P. Bussey⁵⁵, J.M. Butler²⁵, C.M. Buttar⁵⁵, J.M. Butterworth⁹², P. Butti³⁵,
 W. Buttinger³⁵, A. Buzatu¹⁵⁵, A.R. Buzykaev^{120b,120a}, G. Cabras^{23b,23a}, S. Cabrera Urbán¹⁷²,
 D. Caforio¹³⁸, H. Cai¹⁷¹, V.M.M. Cairo², O. Cakir^{4a}, N. Calace⁵², P. Calafiura¹⁸, A. Calandri⁹⁹,
 G. Calderini¹³², P. Calfayan⁶³, G. Callea^{40b,40a}, L.P. Caloba^{78b}, S. Calvente Lopez⁹⁶, D. Calvet³⁷,
 S. Calvet³⁷, T.P. Calvet¹⁵², M. Calvetti^{69a,69b}, R. Camacho Toro³⁶, S. Camarda³⁵, P. Camarri^{71a,71b},
 D. Cameron¹³⁰, R. Caminal Armadans¹⁰⁰, C. Camincher⁵⁶, S. Campana³⁵, M. Campanelli⁹²,
 A. Camplani^{66a,66b}, A. Campoverde¹⁴⁸, V. Canale^{67a,67b}, M. Cano Bret^{58c}, J. Cantero¹²⁵, T. Cao¹⁵⁹,
 Y. Cao¹⁷¹, M.D.M. Capeans Garrido³⁵, I. Caprini^{27b}, M. Caprini^{27b}, M. Capua^{40b,40a}, R.M. Carbone³⁸,
 R. Cardarelli^{71a}, F.C. Cardillo⁵⁰, I. Carli¹³⁹, T. Carli³⁵, G. Carlino^{67a}, B.T. Carlson¹³⁵, L. Carminati^{66a,66b},
 R.M.D. Carney^{43a,43b}, S. Caron¹¹⁷, E. Carquin^{144b}, S. Carrá^{66a,66b}, G.D. Carrillo-Montoya³⁵, D. Casadei^{32b},

M.P. Casado ^{14,g}, A.F. Casha ¹⁶⁵, M. Casolino ¹⁴, D.W. Casper ¹⁶⁹, R. Castelijns ¹¹⁸, V. Castillo Gimenez ¹⁷², N.F. Castro ^{136a,136e}, A. Catinaccio ³⁵, J.R. Catmore ¹³⁰, A. Cattai ³⁵, J. Caudron ²⁴, V. Cavaliere ²⁹, E. Cavallaro ¹⁴, D. Cavalli ^{66a}, M. Cavalli-Sforza ¹⁴, V. Cavasinni ^{69a,69b}, E. Celebi ^{12b}, F. Ceradini ^{72a,72b}, L. Cerda Alberich ¹⁷², A.S. Cerqueira ^{78a}, A. Cerri ¹⁵³, L. Cerrito ^{71a,71b}, F. Cerutti ¹⁸, A. Cervelli ^{23b,23a}, S.A. Cetin ^{12b}, A. Chafaq ^{34a}, D. Chakraborty ¹¹⁹, S.K. Chan ⁵⁷, W.S. Chan ¹¹⁸, Y.L. Chan ^{61a}, P. Chang ¹⁷¹, J.D. Chapman ³¹, D.G. Charlton ²¹, C.C. Chau ³³, C.A. Chavez Barajas ¹⁵³, S. Che ¹²², A. Chegwidan ¹⁰⁴, S. Chekanov ⁶, S.V. Chekulaev ^{166a}, G.A. Chelkov ^{77,at}, M.A. Chelstowska ³⁵, C. Chen ^{58a}, C.H. Chen ⁷⁶, H. Chen ²⁹, J. Chen ^{58a}, J. Chen ³⁸, S. Chen ¹³³, S.J. Chen ^{15c}, X. Chen ^{15b,as}, Y. Chen ⁸⁰, Y.-H. Chen ⁴⁴, H.C. Cheng ¹⁰³, H.J. Cheng ^{15d}, A. Cheplakov ⁷⁷, E. Cheremushkina ¹⁴⁰, R. Cherkaoui El Moursli ^{34e}, E. Cheu ⁷, K. Cheung ⁶², L. Chevalier ¹⁴², V. Chiarella ⁴⁹, G. Chiarelli ^{69a}, G. Chiodini ^{65a}, A.S. Chisholm ³⁵, A. Chitan ^{27b}, I. Chiu ¹⁶¹, Y.H. Chiu ¹⁷⁴, M.V. Chizhov ⁷⁷, K. Choi ⁶³, A.R. Chomont ¹²⁸, S. Chouridou ¹⁶⁰, Y.S. Chow ¹¹⁸, V. Christodoulou ⁹², M.C. Chu ^{61a}, J. Chudoba ¹³⁷, A.J. Chuinard ¹⁰¹, J.J. Chwastowski ⁸², L. Chytka ¹²⁶, D. Cinca ⁴⁵, V. Cindro ⁸⁹, I.A. Cioară ²⁴, A. Ciocio ¹⁸, F. Ciotto ^{67a,67b}, Z.H. Citron ¹⁷⁸, M. Citterio ^{66a}, A. Clark ⁵², M.R. Clark ³⁸, P.J. Clark ⁴⁸, R.N. Clarke ¹⁸, C. Clement ^{43a,43b}, Y. Coadou ⁹⁹, M. Cobal ^{64a,64c}, A. Coccaro ^{53b,53a}, J. Cochran ⁷⁶, A.E.C. Coimbra ¹⁷⁸, L. Colasurdo ¹¹⁷, B. Cole ³⁸, A.P. Colijn ¹¹⁸, J. Collot ⁵⁶, P. Conde Muiño ^{136a,136b}, E. Coniavitis ⁵⁰, S.H. Connell ^{32b}, I.A. Connelly ⁹⁸, S. Constantinescu ^{27b}, F. Conventi ^{67a,av}, A.M. Cooper-Sarkar ¹³¹, F. Cormier ¹⁷³, K.J.R. Cormier ¹⁶⁵, M. Corradi ^{70a,70b}, E.E. Corrigan ⁹⁴, F. Corriveau ^{101,ae}, A. Cortes-Gonzalez ³⁵, M.J. Costa ¹⁷², D. Costanzo ¹⁴⁶, G. Cottin ³¹, G. Cowan ⁹¹, B.E. Cox ⁹⁸, J. Crane ⁹⁸, K. Cranmer ¹²¹, S.J. Crawley ⁵⁵, R.A. Creager ¹³³, G. Cree ³³, S. Crépe-Renaudin ⁵⁶, F. Crescioli ¹³², M. Cristinziani ²⁴, V. Croft ¹²¹, G. Crosetti ^{40b,40a}, A. Cueto ⁹⁶, T. Cuhadar Donszelmann ¹⁴⁶, A.R. Cukierman ¹⁵⁰, M. Curatolo ⁴⁹, J. Cúth ⁹⁷, S. Czekierda ⁸², P. Czodrowski ³⁵, M.J. Da Cunha Sargedas De Sousa ^{58b,136b}, C. Da Via ⁹⁸, W. Dabrowski ^{81a}, T. Dado ^{28a,y}, S. Dahbi ^{34e}, T. Dai ¹⁰³, O. Dale ¹⁷, F. Dallaire ¹⁰⁷, C. Dallapiccola ¹⁰⁰, M. Dam ³⁹, G. D'amen ^{23b,23a}, J.R. Dandoy ¹³³, M.F. Daneri ³⁰, N.P. Dang ^{179,k}, N.D. Dann ⁹⁸, M. Danninger ¹⁷³, V. Dao ³⁵, G. Darbo ^{53b}, S. Darmora ⁸, O. Dartsis ⁵, A. Dattagupta ¹²⁷, T. Daubney ⁴⁴, S. D'Auria ⁵⁵, W. Davey ²⁴, C. David ⁴⁴, T. Davidek ¹³⁹, D.R. Davis ⁴⁷, E. Dawe ¹⁰², I. Dawson ¹⁴⁶, K. De ⁸, R. De Asmundis ^{67a}, A. De Benedetti ¹²⁴, S. De Castro ^{23b,23a}, S. De Cecco ¹³², N. De Groot ¹¹⁷, P. de Jong ¹¹⁸, H. De la Torre ¹⁰⁴, F. De Lorenzi ⁷⁶, A. De Maria ^{51,t}, D. De Pedis ^{70a}, A. De Salvo ^{70a}, U. De Sanctis ^{71a,71b}, A. De Santo ¹⁵³, K. De Vasconcelos Corga ⁹⁹, J.B. De Vivie De Regie ¹²⁸, C. Debenedetti ¹⁴³, D.V. Dedovich ⁷⁷, N. Dehghanian ³, M. Del Gaudio ^{40b,40a}, J. Del Peso ⁹⁶, D. Delgove ¹²⁸, F. Deliot ¹⁴², C.M. Delitzsch ⁷, M. Della Pietra ^{67a,67b}, D. Della Volpe ⁵², A. Dell'Acqua ³⁵, L. Dell'Asta ²⁵, M. Delmastro ⁵, C. Delporte ¹²⁸, P.A. Delsart ⁵⁶, D.A. DeMarco ¹⁶⁵, S. Demers ¹⁸¹, M. Demichev ⁷⁷, S.P. Denisov ¹⁴⁰, D. Denysiuk ¹¹⁸, L. D'Eramo ¹³², D. Derendarz ⁸², J.E. Derkaoui ^{34d}, F. Derue ¹³², P. Dervan ⁸⁸, K. Desch ²⁴, C. Deterre ⁴⁴, K. Dette ¹⁶⁵, M.R. Devesa ³⁰, P.O. Deviveiros ³⁵, A. Dewhurst ¹⁴¹, S. Dhaliwal ²⁶, F.A. Di Bello ⁵², A. Di Ciaccio ^{71a,71b}, L. Di Ciaccio ⁵, W.K. Di Clemente ¹³³, C. Di Donato ^{67a,67b}, A. Di Girolamo ³⁵, B. Di Micco ^{72a,72b}, R. Di Nardo ³⁵, K.F. Di Petrillo ⁵⁷, A. Di Simone ⁵⁰, R. Di Sipio ¹⁶⁵, D. Di Valentino ³³, C. Diaconu ⁹⁹, M. Diamond ¹⁶⁵, F.A. Dias ³⁹, T. Dias Do Vale ^{136a}, M.A. Diaz ^{144a}, J. Dickinson ¹⁸, E.B. Diehl ¹⁰³, J. Dietrich ¹⁹, S. Díez Cornell ⁴⁴, A. Dimitrievska ¹⁸, J. Dingfelder ²⁴, F. Dittus ³⁵, F. Djama ⁹⁹, T. Djobava ^{157b}, J.I. Djuvsland ^{59a}, M.A.B. Do Vale ^{78c}, M. Dobre ^{27b}, D. Dodsworth ²⁶, C. Doglioni ⁹⁴, J. Dolejsi ¹³⁹, Z. Dolezal ¹³⁹, M. Donadelli ^{78d}, J. Donini ³⁷, A. D'Onofrio ⁹⁰, M. D'Onofrio ⁸⁸, J. Dopke ¹⁴¹, A. Doria ^{67a}, M.T. Dova ⁸⁶, A.T. Doyle ⁵⁵, E. Drechsler ⁵¹, E. Dreyer ¹⁴⁹, T. Dreyer ⁵¹, M. Dris ¹⁰, Y. Du ^{58b}, J. Duarte-Campderros ¹⁵⁹, F. Dubinin ¹⁰⁸, A. Dubreuil ⁵², E. Duchovni ¹⁷⁸, G. Duckeck ¹¹², A. Ducourthial ¹³², O.A. Ducu ^{107,x}, D. Duda ¹¹⁸, A. Dudarev ³⁵, A.C. Dudder ⁹⁷, E.M. Duffield ¹⁸, L. Duflot ¹²⁸, M. Dührssen ³⁵, C. Dülse ¹⁸⁰, M. Dumancic ¹⁷⁸, A.E. Dumitriu ^{27b,e}, A.K. Duncan ⁵⁵, M. Dunford ^{59a}, A. Duperrin ⁹⁹, H. Duran Yildiz ^{4a}, M. Düren ⁵⁴, A. Durglishvili ^{157b}, D. Duschinger ⁴⁶, B. Dutta ⁴⁴, D. Duvnjak ¹, M. Dyndal ⁴⁴, B.S. Dziedzic ⁸², C. Eckardt ⁴⁴, K.M. Ecker ¹¹³, R.C. Edgar ¹⁰³, T. Eifert ³⁵, G. Eigen ¹⁷, K. Einsweiler ¹⁸, T. Ekelof ¹⁷⁰, M. El Kacimi ^{34c}, R. El Kosseifi ⁹⁹, V. Ellajosyula ⁹⁹, M. Ellert ¹⁷⁰, F. Ellinghaus ¹⁸⁰, A.A. Elliot ¹⁷⁴, N. Ellis ³⁵, J. Elmsheuser ²⁹, M. Elsing ³⁵, D. Emelianov ¹⁴¹, Y. Enari ¹⁶¹, J.S. Ennis ¹⁷⁶, M.B. Epland ⁴⁷, J. Erdmann ⁴⁵, A. Ereditato ²⁰, S. Errede ¹⁷¹, M. Escalier ¹²⁸, C. Escobar ¹⁷², B. Esposito ⁴⁹, O. Estrada Pastor ¹⁷², A.I. Etienne ¹⁴², E. Etzion ¹⁵⁹, H. Evans ⁶³, A. Ezhilov ¹³⁴, M. Ezzi ^{34e}, F. Fabbri ^{23b,23a}, L. Fabbri ^{23b,23a}, V. Fabiani ¹¹⁷, G. Facini ⁹², R.M. Faisca Rodrigues Pereira ^{136a}, R.M. Fakhruddinov ¹⁴⁰, S. Falciano ^{70a},

P.J. Falke⁵, S. Falke⁵, J. Faltova¹³⁹, Y. Fang^{15a}, M. Fanti^{66a,66b}, A. Farbin⁸, A. Farilla^{72a}, E.M. Farina^{68a,68b}, T. Farooque¹⁰⁴, S. Farrell¹⁸, S.M. Farrington¹⁷⁶, P. Farthouat³⁵, F. Fassi^{34e}, P. Fassnacht³⁵, D. Fassoulidis⁹, M. Faucci Giannelli⁴⁸, A. Favareto^{53b,53a}, W.J. Fawcett⁵², L. Fayard¹²⁸, O.L. Fedin^{134,q}, W. Fedorko¹⁷³, M. Feickert⁴¹, S. Feigl¹³⁰, L. Feligioni⁹⁹, C. Feng^{58b}, E.J. Feng³⁵, M. Feng⁴⁷, M.J. Fenton⁵⁵, A.B. Fenyuk¹⁴⁰, L. Feremenga⁸, J. Ferrando⁴⁴, A. Ferrari¹⁷⁰, P. Ferrari¹¹⁸, R. Ferrari^{68a}, D.E. Ferreira de Lima^{59b}, A. Ferrer¹⁷², D. Ferrere⁵², C. Ferretti¹⁰³, F. Fiedler⁹⁷, A. Filipčič⁸⁹, F. Filthaut¹¹⁷, M. Fincke-Keeler¹⁷⁴, K.D. Finelli²⁵, M.C.N. Fiolhais^{136a,136c,b}, L. Fiorini¹⁷², C. Fischer¹⁴, J. Fischer¹⁸⁰, W.C. Fisher¹⁰⁴, N. Flaschel⁴⁴, I. Fleck¹⁴⁸, P. Fleischmann¹⁰³, R.R.M. Fletcher¹³³, T. Flick¹⁸⁰, B.M. Flierl¹¹², L.M. Flores¹³³, L.R. Flores Castillo^{61a}, N. Fomin¹⁷, G.T. Forcolin⁹⁸, A. Formica¹⁴², F.A. Förster¹⁴, A.C. Forti⁹⁸, A.G. Foster²¹, D. Fournier¹²⁸, H. Fox⁸⁷, S. Fracchia¹⁴⁶, P. Francavilla^{69a,69b}, M. Franchini^{23b,23a}, S. Franchino^{59a}, D. Francis³⁵, L. Franconi¹³⁰, M. Franklin⁵⁷, M. Frate¹⁶⁹, M. Fraternali^{68a,68b}, D. Freeborn⁹², S.M. Fressard-Batraneanu³⁵, B. Freund¹⁰⁷, W.S. Freund^{78b}, D. Froidevaux³⁵, J.A. Frost¹³¹, C. Fukunaga¹⁶², T. Fusayasu¹¹⁴, J. Fuster¹⁷², O. Gabizon¹⁵⁸, A. Gabrielli^{23b,23a}, A. Gabrielli¹⁸, G.P. Gach^{81a}, S. Gadatsch⁵², S. Gadomski⁵², P. Gadow¹¹³, G. Gagliardi^{53b,53a}, L.G. Gagnon¹⁰⁷, C. Galea^{27b}, B. Galhardo^{136a,136c}, E.J. Gallas¹³¹, B.J. Gallop¹⁴¹, P. Gallus¹³⁸, G. Galster³⁹, R. Gamboa Goni⁹⁰, K.K. Gan¹²², S. Ganguly¹⁷⁸, Y. Gao⁸⁸, Y.S. Gao^{150,m}, C. García¹⁷², J.E. García Navarro¹⁷², J.A. García Pascual^{15a}, M. Garcia-Sciveres¹⁸, R.W. Gardner³⁶, N. Garelli¹⁵⁰, V. Garonne¹³⁰, K. Gasnikova⁴⁴, A. Gaudiello^{53b,53a}, G. Gaudio^{68a}, I.L. Gavrilenko¹⁰⁸, A. Gavrilyuk¹⁰⁹, C. Gay¹⁷³, G. Gaycken²⁴, E.N. Gazis¹⁰, C.N.P. Gee¹⁴¹, J. Geisen⁵¹, M. Geisen⁹⁷, M.P. Geisler^{59a}, K. Gellerstedt^{43a,43b}, C. Gemme^{53b}, M.H. Genest⁵⁶, C. Geng¹⁰³, S. Gentile^{70a,70b}, C. Gentsos¹⁶⁰, S. George⁹¹, D. Gerbaudo¹⁴, G. Gessner⁴⁵, S. Ghasemi¹⁴⁸, M. Ghneimat²⁴, B. Giacobbe^{23b}, S. Giagu^{70a,70b}, N. Giangiacomi^{23b,23a}, P. Giannetti^{69a}, S.M. Gibson⁹¹, M. Gignac¹⁴³, D. Gillberg³³, G. Gilles¹⁸⁰, D.M. Gingrich^{3,au}, M.P. Giordani^{64a,64c}, F.M. Giorgi^{23b}, P.F. Giraud¹⁴², P. Giromini⁵⁷, G. Giugliarelli^{64a,64c}, D. Giugni^{66a}, F. Giuliani¹³¹, M. Giulini^{59b}, S. Gkaitatzis¹⁶⁰, I. Gkialas^{9,j}, E.L. Gkoukousis¹⁴, P. Gkoutoumis¹⁰, L.K. Gladilin¹¹¹, C. Glasman⁹⁶, J. Glatzer¹⁴, P.C.F. Glaysher⁴⁴, A. Glazov⁴⁴, M. Goblirsch-Kolb²⁶, J. Godlewski⁸², S. Goldfarb¹⁰², T. Golling⁵², D. Golubkov¹⁴⁰, A. Gomes^{136a,136b,136d}, R. Goncalves Gama^{78a}, R. Gonçalves^{136a}, G. Gonella⁵⁰, L. Gonella²¹, A. Gongadze⁷⁷, F. Gonnella²¹, J.L. Gonski⁵⁷, S. González de la Hoz¹⁷², S. Gonzalez-Sevilla⁵², L. Goossens³⁵, P.A. Gorbounov¹⁰⁹, H.A. Gordon²⁹, B. Gorini³⁵, E. Gorini^{65a,65b}, A. Gorišek⁸⁹, A.T. Goshaw⁴⁷, C. Gössling⁴⁵, M.I. Gostkin⁷⁷, C.A. Gottardo²⁴, C.R. Goudet¹²⁸, D. Goujdami^{34c}, A.G. Goussiou¹⁴⁵, N. Govender^{32b,c}, C. Goy⁵, E. Gozani¹⁵⁸, I. Grabowska-Bold^{81a}, P.O.J. Gradin¹⁷⁰, E.C. Graham⁸⁸, J. Gramling¹⁶⁹, E. Gramstad¹³⁰, S. Grancagnolo¹⁹, V. Gratchev¹³⁴, P.M. Gravila^{27f}, C. Gray⁵⁵, H.M. Gray¹⁸, Z.D. Greenwood^{93,aj}, C. Grefe²⁴, K. Gregersen⁹², I.M. Gregor⁴⁴, P. Grenier¹⁵⁰, K. Grevtsov⁴⁴, J. Griffiths⁸, A.A. Grillo¹⁴³, K. Grimm¹⁵⁰, S. Grinstein^{14,z}, Ph. Gris³⁷, J.-F. Grivaz¹²⁸, S. Groh⁹⁷, E. Gross¹⁷⁸, J. Grosse-Knetter⁵¹, G.C. Grossi⁹³, Z.J. Grout⁹², A. Grummer¹¹⁶, L. Guan¹⁰³, W. Guan¹⁷⁹, J. Guenther³⁵, A. Guerguichon¹²⁸, F. Guescini^{166a}, D. Guest¹⁶⁹, O. Gueta¹⁵⁹, R. Gugel⁵⁰, B. Gui¹²², T. Guillemin⁵, S. Guindon³⁵, U. Gul⁵⁵, C. Gumpert³⁵, J. Guo^{58c}, W. Guo¹⁰³, Y. Guo^{58a,s}, Z. Guo⁹⁹, R. Gupta⁴¹, S. Gurbuz^{12c}, G. Gustavino¹²⁴, B.J. Gutelman¹⁵⁸, P. Gutierrez¹²⁴, N.G. Gutierrez Ortiz⁹², C. Gutschow⁹², C. Guyot¹⁴², M.P. Guzik^{81a}, C. Gwenlan¹³¹, C.B. Gwilliam⁸⁸, A. Haas¹²¹, C. Haber¹⁸, H.K. Hadavand⁸, N. Haddad^{34e}, A. Hadeef⁹⁹, S. Hageböck²⁴, M. Hagihara¹⁶⁷, H. Hakobyan^{182,*}, M. Haleem¹⁷⁵, J. Haley¹²⁵, G. Halladjian¹⁰⁴, G.D. Hallewell⁹⁹, K. Hamacher¹⁸⁰, P. Hamal¹²⁶, K. Hamano¹⁷⁴, A. Hamilton^{32a}, G.N. Hamity¹⁴⁶, K. Han^{58a,ai}, L. Han^{58a}, S. Han^{15d}, K. Hanagaki^{79,v}, M. Hance¹⁴³, D.M. Handl¹¹², B. Haney¹³³, R. Hankache¹³², P. Hanke^{59a}, E. Hansen⁹⁴, J.B. Hansen³⁹, J.D. Hansen³⁹, M.C. Hansen²⁴, P.H. Hansen³⁹, K. Hara¹⁶⁷, A.S. Hard¹⁷⁹, T. Harenberg¹⁸⁰, S. Harkusha¹⁰⁵, P.F. Harrison¹⁷⁶, N.M. Hartmann¹¹², Y. Hasegawa¹⁴⁷, A. Hasib⁴⁸, S. Hassani¹⁴², S. Haug²⁰, R. Hauser¹⁰⁴, L. Hauswald⁴⁶, L.B. Havener³⁸, M. Havranek¹³⁸, C.M. Hawkes²¹, R.J. Hawking³⁵, D. Hayden¹⁰⁴, C. Hayes¹⁵², C.P. Hays¹³¹, J.M. Hays⁹⁰, H.S. Hayward⁸⁸, S.J. Haywood¹⁴¹, M.P. Heath⁴⁸, V. Hedberg⁹⁴, L. Heelan⁸, S. Heer²⁴, K.K. Heidegger⁵⁰, J. Heilman³³, S. Heim⁴⁴, T. Heim¹⁸, B. Heinemann^{44,ap}, J.J. Heinrich¹¹², L. Heinrich¹²¹, C. Heinz⁵⁴, J. Hejbal¹³⁷, L. Helary³⁵, A. Held¹⁷³, S. Hellesund¹³⁰, S. Hellman^{43a,43b}, C. Helsens³⁵, R.C.W. Henderson⁸⁷, Y. Heng¹⁷⁹, S. Henkelmann¹⁷³, A.M. Henriques Correia³⁵, G.H. Herbert¹⁹, H. Herde²⁶, V. Herget¹⁷⁵, Y. Hernández Jiménez^{32c}, H. Herr⁹⁷, G. Herten⁵⁰, R. Hertenberger¹¹², L. Hervas³⁵, T.C. Herwig¹³³,

G.G. Hesketh⁹², N.P. Hessey^{166a}, J.W. Hetherly⁴¹, S. Higashino⁷⁹, E. Higón-Rodríguez¹⁷², K. Hildebrand³⁶, E. Hill¹⁷⁴, J.C. Hill³¹, K.H. Hiller⁴⁴, S.J. Hillier²¹, M. Hils⁴⁶, I. Hinchliffe¹⁸, M. Hirose¹²⁹, D. Hirschbuehl¹⁸⁰, B. Hiti⁸⁹, O. Hladik¹³⁷, D.R. Hlaluku^{32c}, X. Hoad⁴⁸, J. Hobbs¹⁵², N. Hod^{166a}, M.C. Hodgkinson¹⁴⁶, A. Hoecker³⁵, M.R. Hoferkamp¹¹⁶, F. Hoenig¹¹², D. Hohn²⁴, D. Hohov¹²⁸, T.R. Holmes³⁶, M. Holzbock¹¹², M. Homann⁴⁵, S. Honda¹⁶⁷, T. Honda⁷⁹, T.M. Hong¹³⁵, A. Hönle¹¹³, B.H. Hooberman¹⁷¹, W.H. Hopkins¹²⁷, Y. Horii¹¹⁵, P. Horn⁴⁶, A.J. Horton¹⁴⁹, L.A. Horyn³⁶, J.-Y. Hostachy⁵⁶, A. Hostiuc¹⁴⁵, S. Hou¹⁵⁵, A. Hoummada^{34a}, J. Howarth⁹⁸, J. Hoya⁸⁶, M. Hrabovsky¹²⁶, J. Hrdinka³⁵, I. Hristova¹⁹, J. Hrivnac¹²⁸, A. Hrynevich¹⁰⁶, T. Hryn'ova⁵, P.J. Hsu⁶², S.-C. Hsu¹⁴⁵, Q. Hu²⁹, S. Hu^{58c}, Y. Huang^{15a}, Z. Hubacek¹³⁸, F. Hubaut⁹⁹, M. Huebner²⁴, F. Huegging²⁴, T.B. Huffman¹³¹, E.W. Hughes³⁸, M. Huhtinen³⁵, R.F.H. Hunter³³, P. Huo¹⁵², A.M. Hupe³³, N. Huseynov^{77.ag}, J. Huston¹⁰⁴, J. Huth⁵⁷, R. Hyneman¹⁰³, G. Iacobucci⁵², G. Iakovidis²⁹, I. Ibragimov¹⁴⁸, L. Iconomidou-Fayard¹²⁸, Z. Idrissi^{34e}, P. Iengo³⁵, R. Ignazzi³⁹, O. Igonkina^{118.ac}, R. Iguchi¹⁶¹, T. Iizawa¹⁷⁷, Y. Ikegami⁷⁹, M. Ikeno⁷⁹, D. Iliadis¹⁶⁰, N. Ilic¹⁵⁰, F. Iltzsche⁴⁶, G. Introzzi^{68a,68b}, M. Iodice^{72a}, K. Iordanidou³⁸, V. Ippolito^{70a,70b}, M.F. Isacson¹⁷⁰, N. Ishijima¹²⁹, M. Ishino¹⁶¹, M. Ishitsuka¹⁶³, C. Issever¹³¹, S. Istin^{12c.an}, F. Ito¹⁶⁷, J.M. Iturbe Ponce^{61a}, R. Iuppa^{73a,73b}, A. Ivina¹⁷⁸, H. Iwasaki⁷⁹, J.M. Izen⁴², V. Izzo^{67a}, S. Jabbar³, P. Jacka¹³⁷, P. Jackson¹, R.M. Jacobs²⁴, V. Jain², G. Jäkel¹⁸⁰, K.B. Jakobi⁹⁷, K. Jakobs⁵⁰, S. Jakobsen⁷⁴, T. Jakoubek¹³⁷, D.O. Jamin¹²⁵, D.K. Jana⁹³, R. Jansky⁵², J. Janssen²⁴, M. Janus⁵¹, P.A. Janus^{81a}, G. Jarlskog⁹⁴, N. Javadov^{77.ag}, T. Javůrek⁵⁰, M. Javurkova⁵⁰, F. Jeanneau¹⁴², L. Jeanty¹⁸, J. Jejelava^{157a,ah}, A. Jelinskas¹⁷⁶, P. Jenni^{50,d}, J. Jeong⁴⁴, C. Jeske¹⁷⁶, S. Jézéquel⁵, H. Ji¹⁷⁹, J. Jia¹⁵², H. Jiang⁷⁶, Y. Jiang^{58a}, Z. Jiang¹⁵⁰, S. Jiggins⁵⁰, F.A. Jimenez Morales³⁷, J. Jimenez Pena¹⁷², S. Jin^{15c}, A. Jinaru^{27b}, O. Jinnouchi¹⁶³, H. Jivan^{32c}, P. Johansson¹⁴⁶, K.A. Johns⁷, C.A. Johnson⁶³, W.J. Johnson¹⁴⁵, K. Jon-And^{43a,43b}, R.W.L. Jones⁸⁷, S.D. Jones¹⁵³, S. Jones⁷, T.J. Jones⁸⁸, J. Jongmanns^{59a}, P.M. Jorge^{136a,136b}, J. Jovicevic^{166a}, X. Ju¹⁷⁹, J.J. Junggeburth¹¹³, A. Juste Rozas^{14.z}, A. Kaczmarek⁸², M. Kado¹²⁸, H. Kagan¹²², M. Kagan¹⁵⁰, T. Kaji¹⁷⁷, E. Kajomovitz¹⁵⁸, C.W. Kalderon⁹⁴, A. Kaluza⁹⁷, S. Kama⁴¹, A. Kamenshchikov¹⁴⁰, L. Kanjir⁸⁹, Y. Kano¹⁶¹, V.A. Kantserov¹¹⁰, J. Kanzaki⁷⁹, B. Kaplan¹²¹, L.S. Kaplan¹⁷⁹, D. Kar^{32c}, M.J. Kareem^{166b}, E. Karentzos¹⁰, S.N. Karpov⁷⁷, Z.M. Karpova⁷⁷, V. Kartvelishvili⁸⁷, A.N. Karyukhin¹⁴⁰, K. Kasahara¹⁶⁷, L. Kashif¹⁷⁹, R.D. Kass¹²², A. Kastanas¹⁵¹, Y. Kataoka¹⁶¹, C. Kato¹⁶¹, A. Katre⁵², J. Katzy⁴⁴, K. Kawade⁸⁰, K. Kawagoe⁸⁵, T. Kawamoto¹⁶¹, G. Kawamura⁵¹, E.F. Kay⁸⁸, V.F. Kazanin^{120b,120a}, R. Keeler¹⁷⁴, R. Kehoe⁴¹, J.S. Keller³³, E. Kellermann⁹⁴, J.J. Kempster²¹, J. Kendrick²¹, O. Kepka¹³⁷, S. Kersten¹⁸⁰, B.P. Kerševan⁸⁹, R.A. Keyes¹⁰¹, M. Khader¹⁷¹, F. Khalil-Zada¹³, A. Khanov¹²⁵, A.G. Kharlamov^{120b,120a}, T. Kharlamova^{120b,120a}, A. Khodinov¹⁶⁴, T.J. Khoo⁵², V. Khovanskiy^{109,*}, E. Khramov⁷⁷, J. Khubua^{157b}, S. Kido⁸⁰, M. Kiehn⁵², C.R. Kilby⁹¹, H.Y. Kim⁸, S.H. Kim¹⁶⁷, Y.K. Kim³⁶, N. Kimura^{64a,64c}, O.M. Kind¹⁹, B.T. King⁸⁸, D. Kirchmeier⁴⁶, J. Kirk¹⁴¹, A.E. Kiryunin¹¹³, T. Kishimoto¹⁶¹, D. Kisielewska^{81a}, V. Kitali⁴⁴, O. Kivernyk⁵, E. Kladiva^{28b}, T. Klapdor-Kleingrothaus⁵⁰, M.H. Klein¹⁰³, M. Klein⁸⁸, U. Klein⁸⁸, K. Kleinknecht⁹⁷, P. Klimek¹¹⁹, A. Klimentov²⁹, R. Klingenberg^{45,*}, T. Klingl²⁴, T. Klioutchnikova³⁵, F.F. Klitzner¹¹², P. Kluit¹¹⁸, S. Kluth¹¹³, E. Kneringer⁷⁴, E.B.F.G. Knoops⁹⁹, A. Knue⁵⁰, A. Kobayashi¹⁶¹, D. Kobayashi⁸⁵, T. Kobayashi¹⁶¹, M. Kobel⁴⁶, M. Kocian¹⁵⁰, P. Kodys¹³⁹, T. Koffas³³, E. Koffeman¹¹⁸, N.M. Köhler¹¹³, T. Koi¹⁵⁰, M. Kolb^{59b}, I. Koletsou⁵, T. Kondo⁷⁹, N. Kondrashova^{58c}, K. Köneke⁵⁰, A.C. König¹¹⁷, T. Kono^{79,ao}, R. Konoplich^{121.ak}, N. Konstantinidis⁹², B. Konya⁹⁴, R. Kopeliansky⁶³, S. Koperny^{81a}, K. Korcyl⁸², K. Kordas¹⁶⁰, A. Korn⁹², I. Korolkov¹⁴, E.V. Korolkova¹⁴⁶, O. Kortner¹¹³, S. Kortner¹¹³, T. Kosek¹³⁹, V.V. Kostyukhin²⁴, A. Kotwal⁴⁷, A. Koulouris¹⁰, A. Kourkouveli-Charalampidi^{68a,68b}, C. Kourkouvelis⁹, E. Kourlitis¹⁴⁶, V. Kouskoura²⁹, A.B. Kowalewska⁸², R. Kowalewski¹⁷⁴, T.Z. Kowalski^{81a}, C. Kozakai¹⁶¹, W. Kozanecki¹⁴², A.S. Kozhin¹⁴⁰, V.A. Kramarenko¹¹¹, G. Kramberger⁸⁹, D. Krasnopevtsev¹¹⁰, M.W. Krasny¹³², A. Krasznahorkay³⁵, D. Krauss¹¹³, J.A. Kremer^{81a}, J. Kretzschmar⁸⁸, K. Kreutzfeldt⁵⁴, P. Krieger¹⁶⁵, K. Krizka¹⁸, K. Kroeninger⁴⁵, H. Kroha¹¹³, J. Kroll¹³⁷, J. Kroll¹³³, J. Kroseberg²⁴, J. Krstic¹⁶, U. Kruchonak⁷⁷, H. Krüger²⁴, N. Krumnack⁷⁶, M.C. Kruse⁴⁷, T. Kubota¹⁰², S. Kудay^{4b}, J.T. Kuechler¹⁸⁰, S. Kuehn³⁵, A. Kugel^{59a}, F. Kuger¹⁷⁵, T. Kuhl⁴⁴, V. Kukhtin⁷⁷, R. Kukla⁹⁹, Y. Kulchitsky¹⁰⁵, S. Kuleshov^{144b}, Y.P. Kulinich¹⁷¹, M. Kuna⁵⁶, T. Kunigo⁸³, A. Kupco¹³⁷, T. Kupfer⁴⁵, O. Kuprash¹⁵⁹, H. Kurashige⁸⁰, L.L. Kurchaninov^{166a}, Y.A. Kurochkin¹⁰⁵, M.G. Kurth^{15d}, E.S. Kuwertz¹⁷⁴, M. Kuze¹⁶³, J. Kvita¹²⁶, T. Kwan¹⁷⁴, A. La Rosa¹¹³, J.L. La Rosa Navarro^{78d}, L. La Rotonda^{40b,40a}, F. La Ruffa^{40b,40a}, C. Lacasta¹⁷²,

F. Lacava^{70a,70b}, J. Lacey⁴⁴, D.P.J. Lack⁹⁸, H. Lacker¹⁹, D. Lacour¹³², E. Ladygin⁷⁷, R. Lafaye⁵, B. Laforge¹³², S. Lai⁵¹, S. Lammers⁶³, W. Lampl⁷, E. Lançon²⁹, U. Landgraf⁵⁰, M.P.J. Landon⁹⁰, M.C. Lanfermann⁵², V.S. Lang⁴⁴, J.C. Lange¹⁴, R.J. Langenberg³⁵, A.J. Lankford¹⁶⁹, F. Lanni²⁹, K. Lantzscht²⁴, A. Lanza^{68a}, A. Lapertosa^{53b,53a}, S. Laplace¹³², J.F. Laporte¹⁴², T. Lari^{66a}, F. Lasagni Manghi^{23b,23a}, M. Lassnig³⁵, T.S. Lau^{61a}, A. Laudrain¹²⁸, A.T. Law¹⁴³, P. Laycock⁸⁸, M. Lazzaroni^{66a,66b}, B. Le¹⁰², O. Le Dortz¹³², E. Le Guirriec⁹⁹, E.P. Le Quilleuc¹⁴², M. LeBlanc⁷, T. LeCompte⁶, F. Ledroit-Guillon⁵⁶, C.A. Lee²⁹, G.R. Lee^{144a}, L. Lee⁵⁷, S.C. Lee¹⁵⁵, B. Lefebvre¹⁰¹, M. Lefebvre¹⁷⁴, F. Legger¹¹², C. Leggett¹⁸, G. Lehmann Miotto³⁵, W.A. Leight⁴⁴, A. Leisos^{160,w}, M.A.L. Leite^{78d}, R. Leitner¹³⁹, D. Lellouch¹⁷⁸, B. Lemmer⁵¹, K.J.C. Leney⁹², T. Lenz²⁴, B. Lenzi³⁵, R. Leone⁷, S. Leone^{69a}, C. Leonidopoulos⁴⁸, G. Lerner¹⁵³, C. Leroy¹⁰⁷, R. Les¹⁶⁵, A.A.J. Lesage¹⁴², C.G. Lester³¹, M. Levchenko¹³⁴, J. Levêque⁵, D. Levin¹⁰³, L.J. Levinson¹⁷⁸, D. Lewis⁹⁰, B. Li^{58a,s}, C.-Q. Li^{58a}, H. Li^{58b}, L. Li^{58c}, Q. Li^{15d}, Q.Y. Li^{58a}, S. Li^{58d,58c}, X. Li^{58c}, Y. Li¹⁴⁸, Z. Liang^{15a}, B. Liberti^{71a}, A. Liblong¹⁶⁵, K. Lie^{61c}, S. Liem¹¹⁸, A. Limosani¹⁵⁴, C.Y. Lin³¹, K. Lin¹⁰⁴, S.C. Lin¹⁵⁶, T.H. Lin⁹⁷, R.A. Linck⁶³, B.E. Lindquist¹⁵², A.L. Lioni⁵², E. Lipeles¹³³, A. Lipniacka¹⁷, M. Lisovyi^{59b}, T.M. Liss^{171,ar}, A. Lister¹⁷³, A.M. Litke¹⁴³, J.D. Little⁸, B. Liu⁷⁶, B.L. Liu⁶, H.B. Liu²⁹, H. Liu¹⁰³, J.B. Liu^{58a}, J.K.K. Liu¹³¹, K. Liu¹³², M. Liu^{58a}, P. Liu¹⁸, Y.L. Liu^{58a}, Y.W. Liu^{58a}, M. Livan^{68a,68b}, A. Lleres⁵⁶, J. Llorente Merino^{15a}, S.L. Lloyd⁹⁰, C.Y. Lo^{61b}, F. Lo Sterzo⁴¹, E.M. Lobodzinska⁴⁴, P. Loch⁷, F.K. Loebinger⁹⁸, A. Loesle⁵⁰, K.M. Loew²⁶, T. Lohse¹⁹, K. Lohwasser¹⁴⁶, M. Lokajicek¹³⁷, B.A. Long²⁵, J.D. Long¹⁷¹, R.E. Long⁸⁷, L. Longo^{65a,65b}, K.A. Looper¹²², J.A. Lopez^{144b}, I. Lopez Paz¹⁴, A. Lopez Solis¹³², J. Lorenz¹¹², N. Lorenzo Martinez⁵, M. Losada²², P.J. Lösel¹¹², X. Lou⁴⁴, X. Lou^{15a}, A. Lounis¹²⁸, J. Love⁶, P.A. Love⁸⁷, J.J. Lozano Bahilo¹⁷², H. Lu^{61a}, N. Lu¹⁰³, Y.J. Lu⁶², H.J. Lubatti¹⁴⁵, C. Luci^{70a,70b}, A. Lucotte⁵⁶, C. Luedtke⁵⁰, F. Luehring⁶³, I. Luise¹³², W. Lukas⁷⁴, L. Luminari^{70a}, B. Lund-Jensen¹⁵¹, M.S. Lutz¹⁰⁰, P.M. Luzi¹³², D. Lynn²⁹, R. Lysak¹³⁷, E. Lytken⁹⁴, F. Lyu^{15a}, V. Lyubushkin⁷⁷, H. Ma²⁹, L.L. Ma^{58b}, Y. Ma^{58b}, G. Maccarrone⁴⁹, A. Macchiolo¹¹³, C.M. Macdonald¹⁴⁶, J. Machado Miguens^{133,136b}, D. Madaffari¹⁷², R. Madar³⁷, W.F. Mader⁴⁶, A. Madsen⁴⁴, N. Madysa⁴⁶, J. Maeda⁸⁰, S. Maeland¹⁷, T. Maeno²⁹, A.S. Maevskiy¹¹¹, V. Magerl⁵⁰, C. Maidantchik^{78b}, T. Maier¹¹², A. Maio^{136a,136b,136d}, O. Majersky^{28a}, S. Majewski¹²⁷, Y. Makida⁷⁹, N. Makovec¹²⁸, B. Malaescu¹³², Pa. Malecki⁸², V.P. Maleev¹³⁴, F. Malek⁵⁶, U. Mallik⁷⁵, D. Malon⁶, C. Malone³¹, S. Maltezos¹⁰, S. Malyukov³⁵, J. Mamuzic¹⁷², G. Mancini⁴⁹, I. Mandić⁸⁹, J. Maneira^{136a}, L. Manhaes de Andrade Filho^{78a}, J. Manjarres Ramos⁴⁶, K.H. Mankinen⁹⁴, A. Mann¹¹², A. Manousos⁷⁴, B. Mansoulie¹⁴², J.D. Mansour^{15a}, R. Mantifel¹⁰¹, M. Mantoani⁵¹, S. Manzoni^{66a,66b}, G. Marceca³⁰, L. March⁵², L. Marchese¹³¹, G. Marchiori¹³², M. Marcisovsky¹³⁷, C.A. Marin Tobon³⁵, M. Marjanovic³⁷, D.E. Marley¹⁰³, F. Marroquim^{78b}, Z. Marshall¹⁸, M.U.F. Martensson¹⁷⁰, S. Marti-Garcia¹⁷², C.B. Martin¹²², T.A. Martin¹⁷⁶, V.J. Martin⁴⁸, B. Martin dit Latour¹⁷, M. Martinez^{14,z}, V.I. Martinez Outschoorn¹⁰⁰, S. Martin-Haugh¹⁴¹, V.S. Martoiu^{27b}, A.C. Martyniuk⁹², A. Marzin³⁵, L. Masetti⁹⁷, T. Mashimo¹⁶¹, R. Mashinistov¹⁰⁸, J. Masik⁹⁸, A.L. Maslennikov^{120b,120a}, L.H. Mason¹⁰², L. Massa^{71a,71b}, P. Mastrandrea⁵, A. Mastroberardino^{40b,40a}, T. Masubuchi¹⁶¹, P. Mättig¹⁸⁰, J. Maurer^{27b}, B. Maček⁸⁹, S.J. Maxfield⁸⁸, D.A. Maximov^{120b,120a}, R. Mazini¹⁵⁵, I. Maznas¹⁶⁰, S.M. Mazza¹⁴³, N.C. Mc Fadden¹¹⁶, G. Mc Goldrick¹⁶⁵, S.P. Mc Kee¹⁰³, A. McCarn¹⁰³, T.G. McCarthy¹¹³, L.I. McClymont⁹², E.F. McDonald¹⁰², J.A. Mcfayden³⁵, G. Mchedlidze⁵¹, M.A. McKay⁴¹, K.D. McLean¹⁷⁴, S.J. McMahon¹⁴¹, P.C. McNamara¹⁰², C.J. McNicol¹⁷⁶, R.A. McPherson^{174,ae}, J.E. Mdhluli^{32c}, Z.A. Meadows¹⁰⁰, S. Meehan¹⁴⁵, T. Megy⁵⁰, S. Mehlhase¹¹², A. Mehta⁸⁸, T. Meideck⁵⁶, B. Meirose⁴², D. Melini^{172,h}, B.R. Mellado Garcia^{32c}, J.D. Mellenthin⁵¹, M. Melo^{28a}, F. Meloni²⁰, A. Melzer²⁴, S.B. Menary⁹⁸, L. Meng⁸⁸, X.T. Meng¹⁰³, A. Mengarelli^{23b,23a}, S. Menke¹¹³, E. Meoni^{40b,40a}, S. Mergelmeyer¹⁹, C. Merlassino²⁰, P. Mermod⁵², L. Merola^{67a,67b}, C. Meroni^{66a}, F.S. Merritt³⁶, A. Messina^{70a,70b}, J. Metcalfe⁶, A.S. Mete¹⁶⁹, C. Meyer¹³³, J. Meyer¹⁵⁸, J.-P. Meyer¹⁴², H. Meyer Zu Theenhausen^{59a}, F. Miano¹⁵³, R.P. Middleton¹⁴¹, L. Mijović⁴⁸, G. Mikenberg¹⁷⁸, M. Mikestikova¹³⁷, M. Mikuž⁸⁹, M. Milesi¹⁰², A. Milic¹⁶⁵, D.A. Millar⁹⁰, D.W. Miller³⁶, A. Milov¹⁷⁸, D.A. Milstead^{43a,43b}, A.A. Minaenko¹⁴⁰, I.A. Minashvili^{157b}, A.I. Mincer¹²¹, B. Mindur^{81a}, M. Mineev⁷⁷, Y. Minegishi¹⁶¹, Y. Ming¹⁷⁹, L.M. Mir¹⁴, A. Mirto^{65a,65b}, K.P. Mistry¹³³, T. Mitani¹⁷⁷, J. Mitrevski¹¹², V.A. Mitsou¹⁷², A. Miucci²⁰, P.S. Miyagawa¹⁴⁶, A. Mizukami⁷⁹, J.U. Mjörnmark⁹⁴, T. Mkrtchyan¹⁸², M. Mlynarikova¹³⁹, T. Moa^{43a,43b}, K. Mochizuki¹⁰⁷, P. Mogg⁵⁰, S. Mohapatra³⁸, S. Molander^{43a,43b}, R. Moles-Valls²⁴, M.C. Mondragon¹⁰⁴, K. Mönig⁴⁴, J. Monk³⁹, E. Monnier⁹⁹,

A. Montalbano¹⁴⁹, J. Montejo Berlingen³⁵, F. Monticelli⁸⁶, S. Monzani^{66a}, R.W. Moore³, N. Morange¹²⁸, D. Moreno²², M. Moreno Ll  cer³⁵, P. Morettini^{53b}, M. Morgenstern¹¹⁸, S. Morgenstern³⁵, D. Mori¹⁴⁹, T. Mori¹⁶¹, M. Morii⁵⁷, M. Morinaga¹⁷⁷, V. Morisbak¹³⁰, A.K. Morley³⁵, G. Mornacchi³⁵, J.D. Morris⁹⁰, L. Morvaj¹⁵², P. Moschovakos¹⁰, M. Mosidze^{157b}, H.J. Moss¹⁴⁶, J. Moss^{150,n}, K. Motohashi¹⁶³, R. Mount¹⁵⁰, E. Mountricha²⁹, E.J.W. Moyse¹⁰⁰, S. Muanza⁹⁹, F. Mueller¹¹³, J. Mueller¹³⁵, R.S.P. Mueller¹¹², D. Muenstermann⁸⁷, P. Mullen⁵⁵, G.A. Mullier²⁰, F.J. Munoz Sanchez⁹⁸, P. Murin^{28b}, W.J. Murray^{176,141}, A. Murrone^{66a,66b}, M. Mu  skinja⁸⁹, C. Mwewa^{32a}, A.G. Myagkov^{140,al}, J. Myers¹²⁷, M. Myska¹³⁸, B.P. Nachman¹⁸, O. Nackenhorst⁴⁵, K. Nagai¹³¹, R. Nagai^{79,ao}, K. Nagano⁷⁹, Y. Nagasaka⁶⁰, K. Nagata¹⁶⁷, M. Nagel⁵⁰, E. Nagy⁹⁹, A.M. Nairz³⁵, Y. Nakahama¹¹⁵, K. Nakamura⁷⁹, T. Nakamura¹⁶¹, I. Nakano¹²³, F. Napolitano^{59a}, R.F. Naranjo Garcia⁴⁴, R. Narayan¹¹, D.I. Narrias Villar^{59a}, I. Naryshkin¹³⁴, T. Naumann⁴⁴, G. Navarro²², R. Nayyar⁷, H.A. Neal¹⁰³, P.Y. Nechaeva¹⁰⁸, T.J. Neep¹⁴², A. Negri^{68a,68b}, M. Negrini^{23b}, S. Nektarijevic¹¹⁷, C. Nellist⁵¹, M.E. Nelson¹³¹, S. Nemecek¹³⁷, P. Nemethy¹²¹, M. Nessi^{35,f}, M.S. Neubauer¹⁷¹, M. Neumann¹⁸⁰, P.R. Newman²¹, T.Y. Ng^{61c}, Y.S. Ng¹⁹, H.D.N. Nguyen⁹⁹, T. Nguyen Manh¹⁰⁷, E. Nibigira³⁷, R.B. Nickerson¹³¹, R. Nicolaidou¹⁴², J. Nielsen¹⁴³, N. Nikiforou¹¹, V. Nikolaenko^{140,al}, I. Nikolic-Audit¹³², K. Nikolopoulos²¹, P. Nilsson²⁹, Y. Ninomiya⁷⁹, A. Nisati^{70a}, N. Nishu^{58c}, R. Nisius¹¹³, I. Nitsche⁴⁵, T. Nitta¹⁷⁷, T. Nobe¹⁶¹, Y. Noguchi⁸³, M. Nomachi¹²⁹, I. Nomidis³³, M.A. Nomura²⁹, T. Nooney⁹⁰, M. Nordberg³⁵, N. Norjoharuddeen¹³¹, T. Novak⁸⁹, O. Novgorodova⁴⁶, R. Novotny¹³⁸, M. Nozaki⁷⁹, L. Nozka¹²⁶, K. Ntekas¹⁶⁹, E. Nurse⁹², F. Nuti¹⁰², F.G. Oakham^{33,au}, H. Oberlack¹¹³, T. Obermann²⁴, J. Ocariz¹³², A. Ochi⁸⁰, I. Ochoa³⁸, J.P. Ochoa-Ricoux^{144a}, K. O'Connor²⁶, S. Oda⁸⁵, S. Odaka⁷⁹, A. Oh⁹⁸, S.H. Oh⁴⁷, C.C. Ohm¹⁵¹, H. Ohman¹⁷⁰, H. Oide^{53b,53a}, H. Okawa¹⁶⁷, Y. Okazaki⁸³, Y. Okumura¹⁶¹, T. Okuyama⁷⁹, A. Olariu^{27b}, L.F. Oleiro Seabra^{136a}, S.A. Olivares Pino^{144a}, D. Oliveira Damazio²⁹, J.L. Oliver¹, M.J.R. Olsson³⁶, A. Olszewski⁸², J. Olszowska⁸², D.C. O'Neil¹⁴⁹, A. Onofre^{136a,136e}, K. Onogi¹¹⁵, P.U.E. Onyisi¹¹, H. Oppen¹³⁰, M.J. Oreglia³⁶, Y. Oren¹⁵⁹, D. Orestano^{72a,72b}, E.C. Orgill⁹⁸, N. Orlando^{61b}, A.A. O'Rourke⁴⁴, R.S. Orr¹⁶⁵, B. Osculati^{53b,53a,*}, V. O'Shea⁵⁵, R. Ospanov^{58a}, G. Otero y Garzon³⁰, H. Otono⁸⁵, M. Ouchrif^{34d}, F. Ould-Saada¹³⁰, A. Ouraou¹⁴², Q. Ouyang^{15a}, M. Owen⁵⁵, R.E. Owen²¹, V.E. Ozcan^{12c}, N. Ozturk⁸, K. Pachal¹⁴⁹, A. Pacheco Pages¹⁴, L. Pacheco Rodriguez¹⁴², C. Padilla Aranda¹⁴, S. Pagan Griso¹⁸, M. Paganini¹⁸¹, G. Palacino⁶³, S. Palazzo^{40b,40a}, S. Palestini³⁵, M. Palka^{81b}, D. Pallin³⁷, I. Panagoulas¹⁰, C.E. Pandini⁵², J.G. Panduro Vazquez⁹¹, P. Pani³⁵, L. Paolozzi⁵², T.D. Papadopoulou¹⁰, K. Papageorgiou^{9,j}, A. Paramonov⁶, D. Paredes Hernandez^{61b}, B. Parida^{58c}, A.J. Parker⁸⁷, K.A. Parker⁴⁴, M.A. Parker³¹, F. Parodi^{53b,53a}, J.A. Parsons³⁸, U. Parzefall⁵⁰, V.R. Pascuzzi¹⁶⁵, J.M.P. Pasner¹⁴³, E. Pasqualucci^{70a}, S. Passaggio^{53b}, F. Pastore⁹¹, P. Pasuwan^{43a,43b}, S. Pataria⁹⁷, J.R. Pater⁹⁸, A. Pathak^{179,k}, T. Pauly³⁵, B. Pearson¹¹³, M. Pedersen¹³⁰, S. Pedraza Lopez¹⁷², R. Pedro^{136a,136b}, S.V. Peleganchuk^{120b,120a}, O. Penc¹³⁷, C. Peng^{15d}, H. Peng^{58a}, J. Penwell⁶³, B.S. Peralva^{78a}, M.M. Perego¹⁴², A.P. Pereira Peixoto^{136a}, D.V. Perepelitsa²⁹, F. Peri¹⁹, L. Perini^{66a,66b}, H. Pernegger³⁵, S. Perrella^{67a,67b}, V.D. Peshekhonov^{77,*}, K. Peters⁴⁴, R.F.Y. Peters⁹⁸, B.A. Petersen³⁵, T.C. Petersen³⁹, E. Petit⁵⁶, A. Petridis¹, C. Petridou¹⁶⁰, P. Petroff¹²⁸, E. Petrolo^{70a}, M. Petrov¹³¹, F. Petrucci^{72a,72b}, N.E. Pettersson¹⁰⁰, A. Peyaud¹⁴², R. Pezoa^{144b}, T. Pham¹⁰², F.H. Phillips¹⁰⁴, P.W. Phillips¹⁴¹, G. Piacquadio¹⁵², E. Pianori¹⁷⁶, A. Picazio¹⁰⁰, M.A. Pickering¹³¹, R. Piegaia³⁰, J.E. Pilcher³⁶, A.D. Pilkington⁹⁸, M. Pinamonti^{71a,71b}, J.L. Pinfold³, M. Pitt¹⁷⁸, M-A. Pleier²⁹, V. Pleskot¹³⁹, E. Plotnikova⁷⁷, D. Pluth⁷⁶, P. Podberezko^{120b,120a}, R. Poettgen⁹⁴, R. Poggi^{68a,68b}, L. Poggioli¹²⁸, I. Pogrebnyak¹⁰⁴, D. Pohl²⁴, I. Pokharel⁵¹, G. Polesello^{68a}, A. Poley⁴⁴, A. Policicchio^{40b,40a}, R. Polifka³⁵, A. Polini^{23b}, C.S. Pollard⁴⁴, V. Polychronakos²⁹, D. Ponomarenko¹¹⁰, L. Pontecorvo^{70a}, G.A. Popeneciu^{27d}, D.M. Portillo Quintero¹³², S. Pospisil¹³⁸, K. Potamianos⁴⁴, I.N. Potrap⁷⁷, C.J. Potter³¹, H. Potti¹¹, T. Poulsen⁹⁴, J. Poveda³⁵, T.D. Powell¹⁴⁶, M.E. Pozo Astigarraga³⁵, P. Pralavorio⁹⁹, S. Prell⁷⁶, D. Price⁹⁸, M. Primavera^{65a}, S. Prince¹⁰¹, N. Proklova¹¹⁰, K. Prokofiev^{61c}, F. Prokoshin^{144b}, S. Protopopescu²⁹, J. Proudfoot⁶, M. Przybycien^{81a}, A. Puri¹⁷¹, P. Puzo¹²⁸, J. Qian¹⁰³, Y. Qin⁹⁸, A. Quadt⁵¹, M. Queitsch-Maitland⁴⁴, A. Qureshi¹, S.K. Radhakrishnan¹⁵², P. Rados¹⁰², F. Ragusa^{66a,66b}, G. Rahal⁹⁵, J.A. Raine⁹⁸, S. Rajagopalan²⁹, T. Rashid¹²⁸, S. Raspopov⁵, M.G. Ratti^{66a,66b}, D.M. Rauch⁴⁴, F. Rauscher¹¹², S. Rave⁹⁷, B. Ravina¹⁴⁶, I. Ravinovich¹⁷⁸, J.H. Rawling⁹⁸, M. Raymond³⁵, A.L. Read¹³⁰, N.P. Readioff⁵⁶, M. Reale^{65a,65b}, D.M. Rebuzzi^{68a,68b}, A. Redelbach¹⁷⁵, G. Redlinger²⁹, R. Reece¹⁴³, R.G. Reed^{32c}, K. Reeves⁴², L. Rehnisch¹⁹, J. Reichert¹³³, A. Reiss⁹⁷, C. Rembser³⁵,

H. Ren ^{15d}, M. Rescigno ^{70a}, S. Resconi ^{66a}, E.D. Resseguie ¹³³, S. Rettie ¹⁷³, E. Reynolds ²¹,
O.L. Rezanova ^{120b,120a}, P. Reznicek ¹³⁹, R. Richter ¹¹³, S. Richter ⁹², E. Richter-Was ^{81b}, O. Ricken ²⁴,
M. Ridel ¹³², P. Rieck ¹¹³, C.J. Riegel ¹⁸⁰, O. Rifki ⁴⁴, M. Rijssenbeek ¹⁵², A. Rimoldi ^{68a,68b}, M. Rimoldi ²⁰,
L. Rinaldi ^{23b}, G. Ripellino ¹⁵¹, B. Ristić ³⁵, E. Ritsch ³⁵, I. Riu ¹⁴, J.C. Rivera Vergara ^{144a}, F. Rizatdinova ¹²⁵,
E. Rizvi ⁹⁰, C. Rizzi ¹⁴, R.T. Roberts ⁹⁸, S.H. Robertson ^{101,ae}, A. Robichaud-Veronneau ¹⁰¹, D. Robinson ³¹,
J.E.M. Robinson ⁴⁴, A. Robson ⁵⁵, E. Rocco ⁹⁷, C. Roda ^{69a,69b}, Y. Rodina ^{99,aa}, S. Rodriguez Bosca ¹⁷²,
A. Rodriguez Perez ¹⁴, D. Rodriguez Rodriguez ¹⁷², A.M. Rodríguez Vera ^{166b}, S. Roe ³⁵, C.S. Rogan ⁵⁷,
O. Røhne ¹³⁰, R. Röhrig ¹¹³, C.P.A. Roland ⁶³, J. Roloff ⁵⁷, A. Romaniouk ¹¹⁰, M. Romano ^{23b,23a},
E. Romero Adam ¹⁷², N. Rompotis ⁸⁸, M. Ronzani ¹²¹, L. Roos ¹³², S. Rosati ^{70a}, K. Rosbach ⁵⁰, P. Rose ¹⁴³,
N.-A. Rosien ⁵¹, E. Rossi ^{67a,67b}, L.P. Rossi ^{53b}, L. Rossini ^{66a,66b}, J.H.N. Rosten ³¹, R. Rosten ¹⁴⁵, M. Rotaru ^{27b},
J. Rothberg ¹⁴⁵, D. Rousseau ¹²⁸, D. Roy ^{32c}, A. Rozanov ⁹⁹, Y. Rozen ¹⁵⁸, X. Ruan ^{32c}, F. Rubbo ¹⁵⁰,
F. Rühr ⁵⁰, A. Ruiz-Martinez ³³, Z. Rurikova ⁵⁰, N.A. Rusakovich ⁷⁷, H.L. Russell ¹⁰¹, J.P. Rutherford ⁷,
N. Ruthmann ³⁵, E.M. Rüttinger ^{44,l}, Y.F. Ryabov ¹³⁴, M. Rybar ¹⁷¹, G. Rybkin ¹²⁸, S. Ryu ⁶, A. Ryzhov ¹⁴⁰,
G.F. Rzehorz ⁵¹, P. Sabatini ⁵¹, G. Sabato ¹¹⁸, S. Sacerdoti ¹²⁸, H.F.-W. Sadrozinski ¹⁴³, R. Sadykov ⁷⁷,
F. Safai Tehrani ^{70a}, P. Saha ¹¹⁹, M. Sahinsoy ^{59a}, M. Saimpert ⁴⁴, M. Saito ¹⁶¹, T. Saito ¹⁶¹, H. Sakamoto ¹⁶¹,
A. Sakharov ^{121,ak}, D. Salamani ⁵², G. Salamanna ^{72a,72b}, J.E. Salazar Loyola ^{144b}, D. Salek ¹¹⁸,
P.H. Sales De Bruin ¹⁷⁰, D. Salihagic ¹¹³, A. Salnikov ¹⁵⁰, J. Salt ¹⁷², D. Salvatore ^{40b,40a}, F. Salvatore ¹⁵³,
A. Salvucci ^{61a,61b,61c}, A. Salzburger ³⁵, D. Sammel ⁵⁰, D. Sampsonidis ¹⁶⁰, D. Sampsonidou ¹⁶⁰,
J. Sánchez ¹⁷², A. Sanchez Pineda ^{64a,64c}, H. Sandaker ¹³⁰, C.O. Sander ⁴⁴, M. Sandhoff ¹⁸⁰, C. Sandoval ²²,
D.P.C. Sankey ¹⁴¹, M. Sannino ^{53b,53a}, Y. Sano ¹¹⁵, A. Sansoni ⁴⁹, C. Santoni ³⁷, H. Santos ^{136a},
I. Santoyo Castillo ¹⁵³, A. Sapronov ⁷⁷, J.G. Saraiva ^{136a,136d}, O. Sasaki ⁷⁹, K. Sato ¹⁶⁷, E. Sauvan ⁵,
P. Savard ^{165,au}, N. Savic ¹¹³, R. Sawada ¹⁶¹, C. Sawyer ¹⁴¹, L. Sawyer ^{93,aj}, C. Sbarra ^{23b}, A. Sbrizzi ^{23b,23a},
T. Scanlon ⁹², D.A. Scannicchio ¹⁶⁹, J. Schaarschmidt ¹⁴⁵, P. Schacht ¹¹³, B.M. Schachtner ¹¹², D. Schaefer ³⁶,
L. Schaefer ¹³³, J. Schaeffer ⁹⁷, S. Schaepe ³⁵, U. Schäfer ⁹⁷, A.C. Schaffer ¹²⁸, D. Schaile ¹¹²,
R.D. Schamberger ¹⁵², N. Scharmberg ⁹⁸, V.A. Schegelsky ¹³⁴, D. Scheirich ¹³⁹, F. Schenck ¹⁹,
M. Schernau ¹⁶⁹, C. Schiavi ^{53b,53a}, S. Schier ¹⁴³, L.K. Schildgen ²⁴, Z.M. Schillaci ²⁶, E.J. Schioppa ³⁵,
M. Schioppa ^{40b,40a}, K.E. Schleicher ⁵⁰, S. Schlenker ³⁵, K.R. Schmidt-Sommerfeld ¹¹³, K. Schmieden ³⁵,
C. Schmitt ⁹⁷, S. Schmitt ⁴⁴, S. Schmitz ⁹⁷, U. Schnoor ⁵⁰, L. Schoeffel ¹⁴², A. Schoening ^{59b}, E. Schopf ²⁴,
M. Schott ⁹⁷, J.F.P. Schouwenger ¹¹⁷, J. Schovancova ³⁵, S. Schramm ⁵², N. Schuh ⁹⁷, A. Schulte ⁹⁷,
H.-C. Schultz-Coulon ^{59a}, M. Schumacher ⁵⁰, B.A. Schumm ¹⁴³, Ph. Schune ¹⁴², A. Schwartzman ¹⁵⁰,
T.A. Schwarz ¹⁰³, H. Schweiger ⁹⁸, Ph. Schwemling ¹⁴², R. Schwienhorst ¹⁰⁴, A. Sciandra ²⁴, G. Sciolla ²⁶,
M. Scornajenghi ^{40b,40a}, F. Scuri ^{69a}, F. Scutti ¹⁰², L.M. Scyboz ¹¹³, J. Searcy ¹⁰³, C.D. Sebastiani ^{70a,70b},
P. Seema ²⁴, S.C. Seidel ¹¹⁶, A. Seiden ¹⁴³, J.M. Seixas ^{78b}, G. Sekhniaidze ^{67a}, K. Sekhon ¹⁰³, S.J. Sekula ⁴¹,
N. Semprini-Cesari ^{23b,23a}, S. Senkin ³⁷, C. Serfon ¹³⁰, L. Serin ¹²⁸, L. Serkin ^{64a,64b}, M. Sessa ^{72a,72b},
H. Severini ¹²⁴, F. Sforza ¹⁶⁸, A. Sfyrila ⁵², E. Shabalina ⁵¹, J.D. Shahinian ¹⁴³, N.W. Shaikh ^{43a,43b},
L.Y. Shan ^{15a}, R. Shang ¹⁷¹, J.T. Shank ²⁵, M. Shapiro ¹⁸, A.S. Sharma ¹, A. Sharma ¹³¹, P.B. Shatalov ¹⁰⁹,
K. Shaw ^{64a,64b}, S.M. Shaw ⁹⁸, A. Shcherbakova ¹³⁴, C.Y. Shehu ¹⁵³, Y. Shen ¹²⁴, N. Sherafati ³³,
A.D. Sherman ²⁵, P. Sherwood ⁹², L. Shi ^{155,aq}, S. Shimizu ⁸⁰, C.O. Shimmin ¹⁸¹, M. Shimojima ¹¹⁴,
I.P.J. Shipsey ¹³¹, S. Shirabe ⁸⁵, M. Shiyakova ⁷⁷, J. Shlomi ¹⁷⁸, A. Shmeleva ¹⁰⁸, D. Shoaleh Saadi ¹⁰⁷,
M.J. Shochet ³⁶, S. Shojaii ¹⁰², D.R. Shope ¹²⁴, S. Shrestha ¹²², E. Shulga ¹¹⁰, P. Sicho ¹³⁷, A.M. Sickles ¹⁷¹,
P.E. Sidebo ¹⁵¹, E. Sideras Haddad ^{32c}, O. Sidiropoulou ¹⁷⁵, A. Sidoti ^{23b,23a}, F. Siegert ⁴⁶, Dj. Sijacki ¹⁶,
J. Silva ^{136a}, M. Silva Jr. ¹⁷⁹, S.B. Silverstein ^{43a}, L. Simic ⁷⁷, S. Simion ¹²⁸, E. Simioni ⁹⁷, B. Simmons ⁹²,
M. Simon ⁹⁷, P. Sinervo ¹⁶⁵, N.B. Sinev ¹²⁷, M. Sioli ^{23b,23a}, G. Siragusa ¹⁷⁵, I. Siral ¹⁰³, S.Yu. Sivoklov ¹¹¹,
J. Sjölin ^{43a,43b}, M.B. Skinner ⁸⁷, P. Skubic ¹²⁴, M. Slater ²¹, T. Slavicek ¹³⁸, M. Slawinska ⁸², K. Sliwa ¹⁶⁸,
R. Slovak ¹³⁹, V. Smakhtin ¹⁷⁸, B.H. Smart ⁵, J. Smiesko ^{28a}, N. Smirnov ¹¹⁰, S.Yu. Smirnov ¹¹⁰,
Y. Smirnov ¹¹⁰, L.N. Smirnova ¹¹¹, O. Smirnova ⁹⁴, J.W. Smith ⁵¹, M.N.K. Smith ³⁸, R.W. Smith ³⁸,
M. Smizanska ⁸⁷, K. Smolek ¹³⁸, A.A. Snesarev ¹⁰⁸, I.M. Snyder ¹²⁷, S. Snyder ²⁹, R. Sobie ^{174,ae}, F. Socher ⁴⁶,
A.M. Soffa ¹⁶⁹, A. Soffer ¹⁵⁹, A. Søgaard ⁴⁸, D.A. Soh ¹⁵⁵, G. Sokhrannyi ⁸⁹, C.A. Solans Sanchez ³⁵,
M. Solar ¹³⁸, E.Yu. Soldatov ¹¹⁰, U. Soldevila ¹⁷², A.A. Solodkov ¹⁴⁰, A. Soloshenko ⁷⁷, O.V. Solovyanov ¹⁴⁰,
V. Solovyev ¹³⁴, P. Sommer ¹⁴⁶, H. Son ¹⁶⁸, W. Song ¹⁴¹, A. Sopczak ¹³⁸, F. Sopkova ^{28b}, D. Sosa ^{59b},
C.L. Sotiropoulou ^{69a,69b}, S. Sottocornola ^{68a,68b}, R. Soualah ^{64a,64c,i}, A.M. Soukharev ^{120b,120a}, D. South ⁴⁴,
B.C. Sowden ⁹¹, S. Spagnolo ^{65a,65b}, M. Spalla ¹¹³, M. Spangenberg ¹⁷⁶, F. Spanò ⁹¹, D. Sperlich ¹⁹,

F. Spettel¹¹³, T.M. Spieker^{59a}, R. Spighi^{23b}, G. Spigo³⁵, L.A. Spiller¹⁰², M. Spousta¹³⁹, A. Stabile^{66a,66b}, R. Stamen^{59a}, S. Stamm¹⁹, E. Stanecka⁸², R.W. Stanek⁶, C. Stancu^{72a}, M.M. Stanitzki⁴⁴, B.S. Stapf¹¹⁸, S. Stapnes¹³⁰, E.A. Starchenko¹⁴⁰, G.H. Stark³⁶, J. Stark⁵⁶, S.H. Stark³⁹, P. Staroba¹³⁷, P. Starovoitov^{59a}, S. Stärz³⁵, R. Staszewski⁸², M. Stegler⁴⁴, P. Steinberg²⁹, B. Stelzer¹⁴⁹, H.J. Stelzer³⁵, O. Stelzer-Chilton^{166a}, H. Stenzel⁵⁴, T.J. Stevenson⁹⁰, G.A. Stewart⁵⁵, M.C. Stockton¹²⁷, G. Stoicea^{27b}, P. Stolte⁵¹, S. Stonjek¹¹³, A. Straessner⁴⁶, J. Strandberg¹⁵¹, S. Strandberg^{43a,43b}, M. Strauss¹²⁴, P. Strizenec^{28b}, R. Ströhmer¹⁷⁵, D.M. Strom¹²⁷, R. Stroynowski⁴¹, A. Strubig⁴⁸, S.A. Stucci²⁹, B. Stugu¹⁷, J. Stupak¹²⁴, N.A. Styles⁴⁴, D. Su¹⁵⁰, J. Su¹³⁵, S. Suchek^{59a}, Y. Sugaya¹²⁹, M. Suk¹³⁸, V.V. Sulin¹⁰⁸, D.M.S. Sultan⁵², S. Sultansoy^{4c}, T. Sumida⁸³, S. Sun¹⁰³, X. Sun³, K. Suruliz¹⁵³, C.J.E. Suster¹⁵⁴, M.R. Sutton¹⁵³, S. Suzuki⁷⁹, M. Svatos¹³⁷, M. Swiatlowski³⁶, S.P. Swift², A. Sydorenko⁹⁷, I. Sykora^{28a}, T. Sykora¹³⁹, D. Ta⁹⁷, K. Tackmann^{44,ab}, J. Taenzer¹⁵⁹, A. Taffard¹⁶⁹, R. Tahirout^{166a}, E. Tahirovic⁹⁰, N. Taiblum¹⁵⁹, H. Takai²⁹, R. Takashima⁸⁴, E.H. Takasugi¹¹³, K. Takeda⁸⁰, T. Takeshita¹⁴⁷, Y. Takubo⁷⁹, M. Talby⁹⁹, A.A. Talyshev^{120b,120a}, J. Tanaka¹⁶¹, M. Tanaka¹⁶³, R. Tanaka¹²⁸, R. Tanioka⁸⁰, B.B. Tannenwald¹²², S. Tapia Araya^{144b}, S. Tapprogge⁹⁷, A. Tarek Abouelfadl Mohamed¹³², S. Tarem¹⁵⁸, G. Tarna^{27b,e}, G.F. Tartarelli^{66a}, P. Tas¹³⁹, M. Tasevsky¹³⁷, T. Tashiro⁸³, E. Tassi^{40b,40a}, A. Tavares Delgado^{136a,136b}, Y. Tayalati^{34e}, A.C. Taylor¹¹⁶, A.J. Taylor⁴⁸, G.N. Taylor¹⁰², P.T.E. Taylor¹⁰², W. Taylor^{166b}, A.S. Tee⁸⁷, P. Teixeira-Dias⁹¹, D. Temple¹⁴⁹, H. Ten Kate³⁵, P.K. Teng¹⁵⁵, J.J. Teoh¹²⁹, F. Tepel¹⁸⁰, S. Terada⁷⁹, K. Terashi¹⁶¹, J. Terron⁹⁶, S. Terzo¹⁴, M. Testa⁴⁹, R.J. Teuscher^{165,ae}, S.J. Thais¹⁸¹, T. Theveneaux-Pelzer⁴⁴, F. Thiele³⁹, J.P. Thomas²¹, A.S. Thompson⁵⁵, P.D. Thompson²¹, L.A. Thomsen¹⁸¹, E. Thomson¹³³, Y. Tian³⁸, R.E. Ticse Torres⁵¹, V.O. Tikhomirov^{108,am}, Yu.A. Tikhonov^{120b,120a}, S. Timoshenko¹¹⁰, P. Tipton¹⁸¹, S. Tisserant⁹⁹, K. Todome¹⁶³, S. Todorova-Nova⁵, S. Todt⁴⁶, J. Tojo⁸⁵, S. Tokár^{28a}, K. Tokushuku⁷⁹, E. Tolley¹²², M. Tomoto¹¹⁵, L. Tompkins¹⁵⁰, K. Toms¹¹⁶, B. Tong⁵⁷, P. Tornambe⁵⁰, E. Torrence¹²⁷, H. Torres⁴⁶, E. Torró Pastor¹⁴⁵, C. Toscirì¹³¹, J. Toth^{99,ad}, F. Touchard⁹⁹, D.R. Tovey¹⁴⁶, C.J. Treado¹²¹, T. Trefzger¹⁷⁵, F. Tresoldi¹⁵³, A. Tricoli²⁹, I.M. Trigger^{166a}, S. Trincaz-Duvoid¹³², M.F. Tripiana¹⁴, W. Trischuk¹⁶⁵, B. Trocme⁵⁶, A. Trofymov⁴⁴, C. Troncon^{66a}, M. Trovatelli¹⁷⁴, F. Trovato¹⁵³, L. Truong^{32b}, M. Trzebinski⁸², A. Trzupek⁸², F. Tsai⁴⁴, K.W. Tsang^{61a}, J.C.-L. Tseng¹³¹, P.V. Tsiarehsha¹⁰⁵, N. Tsirintanis⁹, S. Tsiskaridze¹⁴, V. Tsiskaridze¹⁵², E.G. Tskhadadze^{157a}, I.I. Tsukerman¹⁰⁹, V. Tsulaia¹⁸, S. Tsuno⁷⁹, D. Tsybychev¹⁵², Y. Tu^{61b}, A. Tudorache^{27b}, V. Tudorache^{27b}, T.T. Tulbure^{27a}, A.N. Tuna⁵⁷, S. Turchikhin⁷⁷, D. Turgeman¹⁷⁸, I. Turk Cakir^{4b,u}, R. Turra^{66a}, P.M. Tuts³⁸, E. Tzovara⁹⁷, G. Uccielli^{23b,23a}, I. Ueda⁷⁹, M. Ughetto^{43a,43b}, F. Ukegawa¹⁶⁷, G. Unal³⁵, A. Undrus²⁹, G. Unel¹⁶⁹, F.C. Ungaro¹⁰², Y. Unno⁷⁹, K. Uno¹⁶¹, J. Urban^{28b}, P. Urquijo¹⁰², P. Urrejola⁹⁷, G. Usai⁸, J. Usui⁷⁹, L. Vacavant⁹⁹, V. Vacek¹³⁸, B. Vachon¹⁰¹, K.O.H. Vadla¹³⁰, A. Vaidya⁹², C. Valderanis¹¹², E. Valdes Santurio^{43a,43b}, M. Valente⁵², S. Valentini^{23b,23a}, A. Valero¹⁷², L. Valéry⁴⁴, R.A. Vallance²¹, A. Vallier⁵, J.A. Valls Ferrer¹⁷², T.R. Van Daalen¹⁴, W. Van Den Wollenberg¹¹⁸, H. Van der Graaf¹¹⁸, P. Van Gemmeren⁶, J. Van Nieuwkoop¹⁴⁹, I. Van Vulpen¹¹⁸, M.C. van Woerden¹¹⁸, M. Vanadia^{71a,71b}, W. Vandelli³⁵, A. Vaniachine¹⁶⁴, P. Vankov¹¹⁸, R. Vari^{70a}, E.W. Varnes⁷, C. Varni^{53b,53a}, T. Varol⁴¹, D. Varouchas¹²⁸, A. Vartapetian⁸, K.E. Varvell¹⁵⁴, G.A. Vasquez^{144b}, J.G. Vasquez¹⁸¹, F. Vazeille³⁷, D. Vazquez Furelos¹⁴, T. Vazquez Schroeder¹⁰¹, J. Veatch⁵¹, V. Vecchio^{72a,72b}, L.M. Veloce¹⁶⁵, F. Veloso^{136a,136c}, S. Veneziano^{70a}, A. Ventura^{65a,65b}, M. Venturi¹⁷⁴, N. Venturi³⁵, V. Vercesi^{68a}, M. Verducci^{72a,72b}, W. Verkerke¹¹⁸, A.T. Vermeulen¹¹⁸, J.C. Vermeulen¹¹⁸, M.C. Vetterli^{149,au}, N. Viaux Maira^{144b}, O. Viazlo⁹⁴, I. Vichou^{171,*}, T. Vickey¹⁴⁶, O.E. Vickey Boeriu¹⁴⁶, G.H.A. Viehhauser¹³¹, S. Viel¹⁸, L. Vignani¹³¹, M. Villa^{23b,23a}, M. Villaplana Perez^{66a,66b}, E. Vilucchi⁴⁹, M.G. Vincker³³, V.B. Vinogradov⁷⁷, A. Vishwakarma⁴⁴, C. Vittori^{23b,23a}, I. Vivarelli¹⁵³, S. Vlachos¹⁰, M. Vogel¹⁸⁰, P. Vokac¹³⁸, G. Volpi¹⁴, S.E. Von Buddenbrock^{32c}, E. Von Toerne²⁴, V. Vorobel¹³⁹, K. Vorobev¹¹⁰, M. Vos¹⁷², J.H. Vosseveld⁸⁸, N. Vranjes¹⁶, M. Vranjes Milosavljevic¹⁶, V. Vrba¹³⁸, M. Vreeswijk¹¹⁸, T. Šfiligoj⁸⁹, R. Vuillermet³⁵, I. Vukotic³⁶, T. Ženiš^{28a}, L. Živković¹⁶, P. Wagner²⁴, W. Wagner¹⁸⁰, J. Wagner-Kuhr¹¹², H. Wahlberg⁸⁶, S. Wahrmund⁴⁶, K. Wakamiya⁸⁰, J. Walder⁸⁷, R. Walker¹¹², W. Walkowiak¹⁴⁸, V. Wallangen^{43a,43b}, A.M. Wang⁵⁷, C. Wang^{58b,e}, F. Wang¹⁷⁹, H. Wang¹⁸, H. Wang³, J. Wang¹⁵⁴, J. Wang^{59b}, P. Wang⁴¹, Q. Wang¹²⁴, R.-J. Wang¹³², R. Wang^{58a}, R. Wang⁶, S.M. Wang¹⁵⁵, T. Wang³⁸, W. Wang^{155,p}, W.X. Wang^{58a,af}, Y. Wang^{58a}, Z. Wang^{58c}, C. Wanotayaroj⁴⁴, A. Warburton¹⁰¹, C.P. Ward³¹, D.R. Wardrope⁹², A. Washbrook⁴⁸, P.M. Watkins²¹,

A.T. Watson²¹, M.F. Watson²¹, G. Watts¹⁴⁵, S. Watts⁹⁸, B.M. Waugh⁹², A.F. Webb¹¹, S. Webb⁹⁷, C. Weber¹⁸¹, M.S. Weber²⁰, S.A. Weber³³, S.M. Weber^{59a}, J.S. Webster⁶, A.R. Weidberg¹³¹, B. Weinert⁶³, J. Weingarten⁵¹, M. Weirich⁹⁷, C. Weiser⁵⁰, P.S. Wells³⁵, T. Wenaus²⁹, T. Wengler³⁵, S. Wenig³⁵, N. Wermes²⁴, M.D. Werner⁷⁶, P. Werner³⁵, M. Wessels^{59a}, T.D. Weston²⁰, K. Whalen¹²⁷, N.L. Whallon¹⁴⁵, A.M. Wharton⁸⁷, A.S. White¹⁰³, A. White⁸, M.J. White¹, R. White^{144b}, D. Whiteson¹⁶⁹, B.W. Whitmore⁸⁷, F.J. Wickens¹⁴¹, W. Wiedenmann¹⁷⁹, M. Wielers¹⁴¹, C. Wigglesworth³⁹, L.A.M. Wiik-Fuchs⁵⁰, A. Wildauer¹¹³, F. Wilk⁹⁸, H.G. Wilkens³⁵, H.H. Williams¹³³, S. Williams³¹, C. Willis¹⁰⁴, S. Willocq¹⁰⁰, J.A. Wilson²¹, I. Wingerter-Seez⁵, E. Winkels¹⁵³, F. Winklmeier¹²⁷, O.J. Winston¹⁵³, B.T. Winter²⁴, M. Wittgen¹⁵⁰, M. Wobisch⁹³, A. Wolf⁹⁷, T.M.H. Wolf¹¹⁸, R. Wolff⁹⁹, M.W. Wolter⁸², H. Wolters^{136a,136c}, V.W.S. Wong¹⁷³, N.L. Woods¹⁴³, S.D. Worm²¹, B.K. Wosiek⁸², K.W. Woźniak⁸², K. Wraight⁵⁵, M. Wu³⁶, S.L. Wu¹⁷⁹, X. Wu⁵², Y. Wu^{58a}, T.R. Wyatt⁹⁸, B.M. Wynne⁴⁸, S. Xella³⁹, Z. Xi¹⁰³, L. Xia^{15b}, D. Xu^{15a}, H. Xu^{58a}, L. Xu²⁹, T. Xu¹⁴², W. Xu¹⁰³, B. Yabsley¹⁵⁴, S. Yacoob^{32a}, K. Yajima¹²⁹, D.P. Yallup⁹², D. Yamaguchi¹⁶³, Y. Yamaguchi¹⁶³, A. Yamamoto⁷⁹, T. Yamanaka¹⁶¹, F. Yamane⁸⁰, M. Yamatani¹⁶¹, T. Yamazaki¹⁶¹, Y. Yamazaki⁸⁰, Z. Yan²⁵, H.J. Yang^{58c,58d}, H.T. Yang¹⁸, S. Yang⁷⁵, Y. Yang¹⁶¹, Y. Yang¹⁵⁵, Z. Yang¹⁷, W.-M. Yao¹⁸, Y.C. Yap⁴⁴, Y. Yasu⁷⁹, E. Yatsenko⁵, K.H. Yau Wong²⁴, J. Ye⁴¹, S. Ye²⁹, I. Yeletsikh⁷⁷, E. Yigitbasi²⁵, E. Yildirim⁹⁷, K. Yorita¹⁷⁷, K. Yoshihara¹³³, C.J.S. Young³⁵, C. Young¹⁵⁰, J. Yu⁸, J. Yu⁷⁶, X. Yue^{59a}, S.P.Y. Yuen²⁴, I. Yusuff^{31,a}, B. Zabinski⁸², G. Zacharis¹⁰, R. Zaidan¹⁴, A.M. Zaitsev^{140,al}, N. Zakharchuk⁴⁴, J. Zalieckas¹⁷, S. Zambito⁵⁷, D. Zanzi³⁵, C. Zeitnitz¹⁸⁰, G. Zemaityte¹³¹, J.C. Zeng¹⁷¹, Q. Zeng¹⁵⁰, O. Zenin¹⁴⁰, D. Zerwas¹²⁸, M. Zgubić¹³¹, D.F. Zhang^{58b}, D. Zhang¹⁰³, F. Zhang¹⁷⁹, G. Zhang^{58a,af}, H. Zhang^{15c}, J. Zhang⁶, L. Zhang⁵⁰, L. Zhang^{58a}, M. Zhang¹⁷¹, P. Zhang^{15c}, R. Zhang^{58a,e}, R. Zhang²⁴, X. Zhang^{58b}, Y. Zhang^{15d}, Z. Zhang¹²⁸, X. Zhao⁴¹, Y. Zhao^{58b,128}, Z. Zhao^{58a}, A. Zhemchugov⁷⁷, B. Zhou¹⁰³, C. Zhou¹⁷⁹, L. Zhou⁴¹, M.S. Zhou^{15d}, M. Zhou¹⁵², N. Zhou^{58c}, Y. Zhou⁷, C.G. Zhu^{58b}, H.L. Zhu^{58a}, H. Zhu^{15a}, J. Zhu¹⁰³, Y. Zhu^{58a}, X. Zhuang^{15a}, K. Zhukov¹⁰⁸, V. Zhulanov^{120b,120a}, A. Zibell¹⁷⁵, D. Zieminska⁶³, N.I. Zimine⁷⁷, S. Zimmermann⁵⁰, Z. Zinonos¹¹³, M. Zinser⁹⁷, M. Ziolkowski¹⁴⁸, G. Zobernig¹⁷⁹, A. Zoccoli^{23b,23a}, K. Zoch⁵¹, T.G. Zorbas¹⁴⁶, R. Zou³⁶, M. Zur Nedden¹⁹, L. Zwalinski³⁵

¹ Department of Physics, University of Adelaide, Adelaide, Australia² Physics Department, SUNY Albany, Albany NY, United States of America³ Department of Physics, University of Alberta, Edmonton AB, Canada⁴ (a) Department of Physics, Ankara University, Ankara; (b) Istanbul Aydin University, Istanbul; (c) Division of Physics, TOBB University of Economics and Technology, Ankara, Turkey⁵ LAPP, Université Grenoble Alpes, Université Savoie Mont Blanc, CNRS/IN2P3, Annecy, France⁶ High Energy Physics Division, Argonne National Laboratory, Argonne IL, United States of America⁷ Department of Physics, University of Arizona, Tucson AZ, United States of America⁸ Department of Physics, University of Texas at Arlington, Arlington TX, United States of America⁹ Physics Department, National and Kapodistrian University of Athens, Athens, Greece¹⁰ Physics Department, National Technical University of Athens, Zografou, Greece¹¹ Department of Physics, University of Texas at Austin, Austin TX, United States of America¹² (a) Bahcesehir University, Faculty of Engineering and Natural Sciences, Istanbul; (b) Istanbul Bilgi University, Faculty of Engineering and Natural Sciences, Istanbul; (c) Department of Physics, Bogazici University, Istanbul; (d) Department of Physics Engineering, Gaziantep University, Gaziantep, Turkey¹³ Institute of Physics, Azerbaijan Academy of Sciences, Baku, Azerbaijan¹⁴ Institut de Física d'Altes Energies (IFAE), Barcelona Institute of Science and Technology, Barcelona, Spain¹⁵ (a) Institute of High Energy Physics, Chinese Academy of Sciences, Beijing; (b) Physics Department, Tsinghua University, Beijing; (c) Department of Physics, Nanjing University, Nanjing;

(d) University of Chinese Academy of Science (UCAS), Beijing, China

¹⁶ Institute of Physics, University of Belgrade, Belgrade, Serbia¹⁷ Department for Physics and Technology, University of Bergen, Bergen, Norway¹⁸ Physics Division, Lawrence Berkeley National Laboratory and University of California, Berkeley CA, United States of America¹⁹ Institut für Physik, Humboldt Universität zu Berlin, Berlin, Germany²⁰ Albert Einstein Center for Fundamental Physics and Laboratory for High Energy Physics, University of Bern, Bern, Switzerland²¹ School of Physics and Astronomy, University of Birmingham, Birmingham, United Kingdom²² Centro de Investigaciones, Universidad Antonio Nariño, Bogota, Colombia²³ (a) Dipartimento di Fisica e Astronomia, Università di Bologna, Bologna; (b) INFN Sezione di Bologna, Italy²⁴ Physikalisches Institut, Universität Bonn, Bonn, Germany²⁵ Department of Physics, Boston University, Boston MA, United States of America²⁶ Department of Physics, Brandeis University, Waltham MA, United States of America²⁷ (a) Transilvania University of Brasov, Brasov; (b) Horia Hulubei National Institute of Physics and Nuclear Engineering, Bucharest; (c) Department of Physics, Alexandru Ioan Cuza University of Iasi, Iasi; (d) National Institute for Research and Development of Isotopic and Molecular Technologies, Physics Department, Cluj-Napoca; (e) University Politehnica Bucharest, Bucharest; (f) West University in Timisoara, Timisoara, Romania²⁸ (a) Faculty of Mathematics, Physics and Informatics, Comenius University, Bratislava; (b) Department of Subnuclear Physics, Institute of Experimental Physics of the Slovak Academy of Sciences, Kosice, Slovak Republic²⁹ Physics Department, Brookhaven National Laboratory, Upton NY, United States of America³⁰ Departamento de Física, Universidad de Buenos Aires, Buenos Aires, Argentina³¹ Cavendish Laboratory, University of Cambridge, Cambridge, United Kingdom³² (a) Department of Physics, University of Cape Town, Cape Town; (b) Department of Mechanical Engineering Science, University of Johannesburg, Johannesburg; (c) School of Physics, University of the Witwatersrand, Johannesburg, South Africa³³ Department of Physics, Carleton University, Ottawa ON, Canada

- ³⁴ ^(a) Faculté des Sciences Ain Chock, Réseau Universitaire de Physique des Hautes Energies - Université Hassan II, Casablanca; ^(b) Centre National de l'Energie des Sciences Techniques Nucleaires (CNSTEN), Rabat; ^(c) Faculté des Sciences Semlalia, Université Cadi Ayyad, LPHEA-Marrakech; ^(d) Faculté des Sciences, Université Mohamed Premier and LPTPM, Oujda;
- ^(e) Faculté des sciences, Université Mohammed V, Rabat, Morocco
- ³⁵ CERN, Geneva, Switzerland
- ³⁶ Enrico Fermi Institute, University of Chicago, Chicago IL, United States of America
- ³⁷ LPC, Université Clermont Auvergne, CNRS/IN2P3, Clermont-Ferrand, France
- ³⁸ Nevis Laboratory, Columbia University, Irvington NY, United States of America
- ³⁹ Niels Bohr Institute, University of Copenhagen, Copenhagen, Denmark
- ⁴⁰ ^(a) Dipartimento di Fisica, Università della Calabria, Rende; ^(b) INFN Gruppo Collegato di Cosenza, Laboratori Nazionali di Frascati, Italy
- ⁴¹ Physics Department, Southern Methodist University, Dallas TX, United States of America
- ⁴² Physics Department, University of Texas at Dallas, Richardson TX, United States of America
- ⁴³ ^(a) Department of Physics, Stockholm University; ^(b) Oskar Klein Centre, Stockholm, Sweden
- ⁴⁴ Deutsches Elektronen-Synchrotron DESY, Hamburg and Zeuthen, Germany
- ⁴⁵ Lehrstuhl für Experimentelle Physik IV, Technische Universität Dortmund, Dortmund, Germany
- ⁴⁶ Institut für Kern- und Teilchenphysik, Technische Universität Dresden, Dresden, Germany
- ⁴⁷ Department of Physics, Duke University, Durham NC, United States of America
- ⁴⁸ SUPA - School of Physics and Astronomy, University of Edinburgh, Edinburgh, United Kingdom
- ⁴⁹ INFN e Laboratori Nazionali di Frascati, Frascati, Italy
- ⁵⁰ Physikalisches Institut, Albert-Ludwigs-Universität Freiburg, Freiburg, Germany
- ⁵¹ II. Physikalisches Institut, Georg-August-Universität Göttingen, Göttingen, Germany
- ⁵² Département de Physique Nucléaire et Corpusculaire, Université de Genève, Genève, Switzerland
- ⁵³ ^(a) Dipartimento di Fisica, Università di Genova, Genova; ^(b) INFN Sezione di Genova, Italy
- ⁵⁴ II. Physikalisches Institut, Justus-Liebig-Universität Giessen, Giessen, Germany
- ⁵⁵ SUPA - School of Physics and Astronomy, University of Glasgow, Glasgow, United Kingdom
- ⁵⁶ LPSC, Université Grenoble Alpes, CNRS/IN2P3, Grenoble INP, Grenoble, France
- ⁵⁷ Laboratory for Particle Physics and Cosmology, Harvard University, Cambridge MA, United States of America
- ⁵⁸ ^(a) Department of Modern Physics and State Key Laboratory of Particle Detection and Electronics, University of Science and Technology of China, Hefei; ^(b) Institute of Frontier and Interdisciplinary Science and Key Laboratory of Particle Physics and Particle Irradiation (MOE), Shandong University, Qingdao; ^(c) School of Physics and Astronomy, Shanghai Jiao Tong University, KLPPAC-MOE, SKLPPC, Shanghai; ^(d) Tsung-Dao Lee Institute, Shanghai, China
- ⁵⁹ ^(a) Kirchhoff-Institut für Physik, Ruprecht-Karls-Universität Heidelberg, Heidelberg; ^(b) Physikalisches Institut, Ruprecht-Karls-Universität Heidelberg, Heidelberg, Germany
- ⁶⁰ Faculty of Applied Information Science, Hiroshima Institute of Technology, Hiroshima, Japan
- ⁶¹ ^(a) Department of Physics, Chinese University of Hong Kong, Shatin, N.T., Hong Kong; ^(b) Department of Physics, University of Hong Kong, Hong Kong; ^(c) Department of Physics and Institute for Advanced Study, Hong Kong University of Science and Technology, Clear Water Bay, Kowloon, Hong Kong, China
- ⁶² Department of Physics, National Tsing Hua University, Hsinchu, Taiwan
- ⁶³ Department of Physics, Indiana University, Bloomington IN, United States of America
- ⁶⁴ ^(a) INFN Gruppo Collegato di Udine, Sezione di Trieste, Udine; ^(b) ICTP, Trieste; ^(c) Dipartimento di Chimica, Fisica e Ambiente, Università di Udine, Udine, Italy
- ⁶⁵ ^(a) INFN Sezione di Lecce; ^(b) Dipartimento di Matematica e Fisica, Università del Salento, Lecce, Italy
- ⁶⁶ ^(a) INFN Sezione di Milano; ^(b) Dipartimento di Fisica, Università di Milano, Milano, Italy
- ⁶⁷ ^(a) INFN Sezione di Napoli; ^(b) Dipartimento di Fisica, Università di Napoli, Napoli, Italy
- ⁶⁸ ^(a) INFN Sezione di Pavia; ^(b) Dipartimento di Fisica, Università di Pavia, Pavia, Italy
- ⁶⁹ ^(a) INFN Sezione di Pisa; ^(b) Dipartimento di Fisica E. Fermi, Università di Pisa, Pisa, Italy
- ⁷⁰ ^(a) INFN Sezione di Roma; ^(b) Dipartimento di Fisica, Sapienza Università di Roma, Roma, Italy
- ⁷¹ ^(a) INFN Sezione di Roma Tor Vergata; ^(b) Dipartimento di Fisica, Università di Roma Tor Vergata, Roma, Italy
- ⁷² ^(a) INFN Sezione di Roma Tre; ^(b) Dipartimento di Matematica e Fisica, Università Roma Tre, Roma, Italy
- ⁷³ ^(a) INFN-TIFPA; ^(b) Università degli Studi di Trento, Trento, Italy
- ⁷⁴ Institut für Astro- und Teilchenphysik, Leopold-Franzens-Universität, Innsbruck, Austria
- ⁷⁵ University of Iowa, Iowa City IA, United States of America
- ⁷⁶ Department of Physics and Astronomy, Iowa State University, Ames IA, United States of America
- ⁷⁷ Joint Institute for Nuclear Research, Dubna, Russia
- ⁷⁸ ^(a) Departamento de Engenharia Elétrica, Universidade Federal de Juiz de Fora (UFJF), Juiz de Fora; ^(b) Universidade Federal do Rio De Janeiro COPPE/EE/IF, Rio de Janeiro; ^(c) Universidade Federal de São João del Rei (UFSJ), São João del Rei; ^(d) Instituto de Física, Universidade de São Paulo, São Paulo, Brazil
- ⁷⁹ KEK, High Energy Accelerator Research Organization, Tsukuba, Japan
- ⁸⁰ Graduate School of Science, Kobe University, Kobe, Japan
- ⁸¹ ^(a) AGH University of Science and Technology, Faculty of Physics and Applied Computer Science, Krakow; ^(b) Marian Smoluchowski Institute of Physics, Jagiellonian University, Krakow, Poland
- ⁸² Institute of Nuclear Physics Polish Academy of Sciences, Krakow, Poland
- ⁸³ Faculty of Science, Kyoto University, Kyoto, Japan
- ⁸⁴ Kyoto University of Education, Kyoto, Japan
- ⁸⁵ Research Center for Advanced Particle Physics and Department of Physics, Kyushu University, Fukuoka, Japan
- ⁸⁶ Instituto de Física La Plata, Universidad Nacional de La Plata and CONICET, La Plata, Argentina
- ⁸⁷ Physics Department, Lancaster University, Lancaster, United Kingdom
- ⁸⁸ Oliver Lodge Laboratory, University of Liverpool, Liverpool, United Kingdom
- ⁸⁹ Department of Experimental Particle Physics, Jožef Stefan Institute and Department of Physics, University of Ljubljana, Ljubljana, Slovenia
- ⁹⁰ School of Physics and Astronomy, Queen Mary University of London, London, United Kingdom
- ⁹¹ Department of Physics, Royal Holloway University of London, Egham, United Kingdom
- ⁹² Department of Physics and Astronomy, University College London, London, United Kingdom
- ⁹³ Louisiana Tech University, Ruston LA, United States of America
- ⁹⁴ Fysiska institutionen, Lunds universitet, Lund, Sweden
- ⁹⁵ Centre de Calcul de l'Institut National de Physique Nucléaire et de Physique des Particules (IN2P3), Villeurbanne, France
- ⁹⁶ Departamento de Física Teórica C-15 and CIAFF, Universidad Autónoma de Madrid, Madrid, Spain
- ⁹⁷ Institut für Physik, Universität Mainz, Mainz, Germany
- ⁹⁸ School of Physics and Astronomy, University of Manchester, Manchester, United Kingdom
- ⁹⁹ CPPM, Aix-Marseille Université, CNRS/IN2P3, Marseille, France
- ¹⁰⁰ Department of Physics, University of Massachusetts, Amherst MA, United States of America
- ¹⁰¹ Department of Physics, McGill University, Montreal QC, Canada
- ¹⁰² School of Physics, University of Melbourne, Victoria, Australia
- ¹⁰³ Department of Physics, University of Michigan, Ann Arbor MI, United States of America
- ¹⁰⁴ Department of Physics and Astronomy, Michigan State University, East Lansing MI, United States of America
- ¹⁰⁵ B.I. Stepanov Institute of Physics, National Academy of Sciences of Belarus, Minsk, Belarus

- ¹⁰⁶ Research Institute for Nuclear Problems of Byelorussian State University, Minsk, Belarus
- ¹⁰⁷ Group of Particle Physics, University of Montreal, Montreal QC, Canada
- ¹⁰⁸ P.N. Lebedev Physical Institute of the Russian Academy of Sciences, Moscow, Russia
- ¹⁰⁹ Institute for Theoretical and Experimental Physics (ITEP), Moscow, Russia
- ¹¹⁰ National Research Nuclear University MEPhI, Moscow, Russia
- ¹¹¹ D.V. Skobeltsyn Institute of Nuclear Physics, M.V. Lomonosov Moscow State University, Moscow, Russia
- ¹¹² Fakultät für Physik, Ludwig-Maximilians-Universität München, München, Germany
- ¹¹³ Max-Planck-Institut für Physik (Werner-Heisenberg-Institut), München, Germany
- ¹¹⁴ Nagasaki Institute of Applied Science, Nagasaki, Japan
- ¹¹⁵ Graduate School of Science and Kobayashi-Maskawa Institute, Nagoya University, Nagoya, Japan
- ¹¹⁶ Department of Physics and Astronomy, University of New Mexico, Albuquerque NM, United States of America
- ¹¹⁷ Institute for Mathematics, Astrophysics and Particle Physics, Radboud University Nijmegen/Nikhef, Nijmegen, Netherlands
- ¹¹⁸ Nikhef National Institute for Subatomic Physics and University of Amsterdam, Amsterdam, Netherlands
- ¹¹⁹ Department of Physics, Northern Illinois University, DeKalb IL, United States of America
- ¹²⁰ ^(a) Budker Institute of Nuclear Physics, SB RAS, Novosibirsk; ^(b) Novosibirsk State University Novosibirsk, Russia
- ¹²¹ Department of Physics, New York University, New York NY, United States of America
- ¹²² Ohio State University, Columbus OH, United States of America
- ¹²³ Faculty of Science, Okayama University, Okayama, Japan
- ¹²⁴ Homer L. Dodge Department of Physics and Astronomy, University of Oklahoma, Norman OK, United States of America
- ¹²⁵ Department of Physics, Oklahoma State University, Stillwater OK, United States of America
- ¹²⁶ Palacký University, RCPTM, Joint Laboratory of Optics, Olomouc, Czech Republic
- ¹²⁷ Center for High Energy Physics, University of Oregon, Eugene OR, United States of America
- ¹²⁸ LAL, Université Paris-Sud, CNRS/IN2P3, Université Paris-Saclay, Orsay, France
- ¹²⁹ Graduate School of Science, Osaka University, Osaka, Japan
- ¹³⁰ Department of Physics, University of Oslo, Oslo, Norway
- ¹³¹ Department of Physics, Oxford University, Oxford, United Kingdom
- ¹³² LPNHE, Sorbonne Université, Paris Diderot Sorbonne Paris Cité, CNRS/IN2P3, Paris, France
- ¹³³ Department of Physics, University of Pennsylvania, Philadelphia PA, United States of America
- ¹³⁴ Konstantinov Nuclear Physics Institute of National Research Centre "Kurchatov Institute", PNPI, St. Petersburg, Russia
- ¹³⁵ Department of Physics and Astronomy, University of Pittsburgh, Pittsburgh PA, United States of America
- ¹³⁶ ^(a) Laboratório de Instrumentação e Física Experimental de Partículas - LIP; ^(b) Departamento de Física, Faculdade de Ciências, Universidade de Lisboa, Lisboa; ^(c) Departamento de Física, Universidade de Coimbra, Coimbra; ^(d) Centro de Física Nuclear da Universidade de Lisboa, Lisboa; ^(e) Departamento de Física, Universidade do Minho, Braga; ^(f) Departamento de Física Teórica y del Cosmos, Universidad de Granada, Granada (Spain); ^(g) Dep Física and CEFITEC of Faculdade de Ciências e Tecnologia, Universidade Nova de Lisboa, Caparica, Portugal
- ¹³⁷ Institute of Physics, Academy of Sciences of the Czech Republic, Prague, Czech Republic
- ¹³⁸ Czech Technical University in Prague, Prague, Czech Republic
- ¹³⁹ Charles University, Faculty of Mathematics and Physics, Prague, Czech Republic
- ¹⁴⁰ State Research Center Institute for High Energy Physics, NRC KI, Protvino, Russia
- ¹⁴¹ Particle Physics Department, Rutherford Appleton Laboratory, Didcot, United Kingdom
- ¹⁴² IRFU, CEA, Université Paris-Saclay, Gif-sur-Yvette, France
- ¹⁴³ Santa Cruz Institute for Particle Physics, University of California Santa Cruz, Santa Cruz CA, United States of America
- ¹⁴⁴ ^(a) Departamento de Física, Pontificia Universidad Católica de Chile, Santiago; ^(b) Departamento de Física, Universidad Técnica Federico Santa María, Valparaíso, Chile
- ¹⁴⁵ Department of Physics, University of Washington, Seattle WA, United States of America
- ¹⁴⁶ Department of Physics and Astronomy, University of Sheffield, Sheffield, United Kingdom
- ¹⁴⁷ Department of Physics, Shinshu University, Nagano, Japan
- ¹⁴⁸ Department Physik, Universität Siegen, Siegen, Germany
- ¹⁴⁹ Department of Physics, Simon Fraser University, Burnaby BC, Canada
- ¹⁵⁰ SLAC National Accelerator Laboratory, Stanford CA, United States of America
- ¹⁵¹ Physics Department, Royal Institute of Technology, Stockholm, Sweden
- ¹⁵² Departments of Physics and Astronomy, Stony Brook University, Stony Brook NY, United States of America
- ¹⁵³ Department of Physics and Astronomy, University of Sussex, Brighton, United Kingdom
- ¹⁵⁴ School of Physics, University of Sydney, Sydney, Australia
- ¹⁵⁵ Institute of Physics, Academia Sinica, Taipei, Taiwan
- ¹⁵⁶ Academia Sinica Grid Computing, Institute of Physics, Academia Sinica, Taipei, Taiwan
- ¹⁵⁷ ^(a) E. Andronikashvili Institute of Physics, Iv. Javakishvili Tbilisi State University, Tbilisi; ^(b) High Energy Physics Institute, Tbilisi State University, Tbilisi, Georgia
- ¹⁵⁸ Department of Physics, Technion, Israel Institute of Technology, Haifa, Israel
- ¹⁵⁹ Raymond and Beverly Sackler School of Physics and Astronomy, Tel Aviv University, Tel Aviv, Israel
- ¹⁶⁰ Department of Physics, Aristotle University of Thessaloniki, Thessaloniki, Greece
- ¹⁶¹ International Center for Elementary Particle Physics and Department of Physics, University of Tokyo, Tokyo, Japan
- ¹⁶² Graduate School of Science and Technology, Tokyo Metropolitan University, Tokyo, Japan
- ¹⁶³ Department of Physics, Tokyo Institute of Technology, Tokyo, Japan
- ¹⁶⁴ Tomsk State University, Tomsk, Russia
- ¹⁶⁵ Department of Physics, University of Toronto, Toronto ON, Canada
- ¹⁶⁶ ^(a) TRIUMF, Vancouver BC; ^(b) Department of Physics and Astronomy, York University, Toronto ON, Canada
- ¹⁶⁷ Division of Physics and Tomonaga Center for the History of the Universe, Faculty of Pure and Applied Sciences, University of Tsukuba, Tsukuba, Japan
- ¹⁶⁸ Department of Physics and Astronomy, Tufts University, Medford MA, United States of America
- ¹⁶⁹ Department of Physics and Astronomy, University of California Irvine, Irvine CA, United States of America
- ¹⁷⁰ Department of Physics and Astronomy, University of Uppsala, Uppsala, Sweden
- ¹⁷¹ Department of Physics, University of Illinois, Urbana IL, United States of America
- ¹⁷² Instituto de Física Corpuscular (IFIC), Centro Mixto Universidad de Valencia - CSIC, Valencia, Spain
- ¹⁷³ Department of Physics, University of British Columbia, Vancouver BC, Canada
- ¹⁷⁴ Department of Physics and Astronomy, University of Victoria, Victoria BC, Canada
- ¹⁷⁵ Fakultät für Physik und Astronomie, Julius-Maximilians-Universität Würzburg, Würzburg, Germany
- ¹⁷⁶ Department of Physics, University of Warwick, Coventry, United Kingdom
- ¹⁷⁷ Waseda University, Tokyo, Japan
- ¹⁷⁸ Department of Particle Physics, Weizmann Institute of Science, Rehovot, Israel
- ¹⁷⁹ Department of Physics, University of Wisconsin, Madison WI, United States of America
- ¹⁸⁰ Fakultät für Mathematik und Naturwissenschaften, Fachgruppe Physik, Bergische Universität Wuppertal, Wuppertal, Germany
- ¹⁸¹ Department of Physics, Yale University, New Haven CT, United States of America
- ¹⁸² Yerevan Physics Institute, Yerevan, Armenia

- ^a Also at Department of Physics, University of Malaya, Kuala Lumpur; Malaysia.
- ^b Also at Borough of Manhattan Community College, City University of New York, NY; United States of America.
- ^c Also at Centre for High Performance Computing, CSIR Campus, Rosebank, Cape Town; South Africa.
- ^d Also at CERN, Geneva; Switzerland.
- ^e Also at CPPM, Aix-Marseille Université, CNRS/IN2P3, Marseille; France.
- ^f Also at Département de Physique Nucléaire et Corpusculaire, Université de Genève, Genève; Switzerland.
- ^g Also at Departament de Física de la Universitat Autònoma de Barcelona, Barcelona; Spain.
- ^h Also at Departamento de Física Teórica y del Cosmos, Universidad de Granada, Granada (Spain); Spain.
- ⁱ Also at Department of Applied Physics and Astronomy, University of Sharjah, Sharjah; United Arab Emirates.
- ^j Also at Department of Financial and Management Engineering, University of the Aegean, Chios; Greece.
- ^k Also at Department of Physics and Astronomy, University of Louisville, Louisville, KY; United States of America.
- ^l Also at Department of Physics and Astronomy, University of Sheffield, Sheffield; United Kingdom.
- ^m Also at Department of Physics, California State University, Fresno CA; United States of America.
- ⁿ Also at Department of Physics, California State University, Sacramento CA; United States of America.
- ^o Also at Department of Physics, King's College London, London; United Kingdom.
- ^p Also at Department of Physics, Nanjing University, Nanjing; China.
- ^q Also at Department of Physics, St. Petersburg State Polytechnical University, St. Petersburg; Russia.
- ^r Also at Department of Physics, University of Fribourg, Fribourg; Switzerland.
- ^s Also at Department of Physics, University of Michigan, Ann Arbor MI; United States of America.
- ^t Also at Dipartimento di Fisica E. Fermi, Università di Pisa, Pisa; Italy.
- ^u Also at Giresun University, Faculty of Engineering, Giresun; Turkey.
- ^v Also at Graduate School of Science, Osaka University, Osaka; Japan.
- ^w Also at Hellenic Open University, Patras; Greece.
- ^x Also at Horia Hulubei National Institute of Physics and Nuclear Engineering, Bucharest; Romania.
- ^y Also at II. Physikalisches Institut, Georg-August-Universität Göttingen, Göttingen; Germany.
- ^z Also at Institut Catalana de Recerca i Estudis Avançats, ICREA, Barcelona; Spain.
- ^{aa} Also at Institut de Física d'Altes Energies (IFAE), Barcelona Institute of Science and Technology, Barcelona; Spain.
- ^{ab} Also at Institut für Experimentalphysik, Universität Hamburg, Hamburg; Germany.
- ^{ac} Also at Institute for Mathematics, Astrophysics and Particle Physics, Radboud University Nijmegen/Nikhef, Nijmegen; Netherlands.
- ^{ad} Also at Institute for Particle and Nuclear Physics, Wigner Research Centre for Physics, Budapest; Hungary.
- ^{ae} Also at Institute of Particle Physics (IPP); Canada.
- ^{af} Also at Institute of Physics, Academia Sinica, Taipei; Taiwan.
- ^{ag} Also at Institute of Physics, Azerbaijan Academy of Sciences, Baku; Azerbaijan.
- ^{ah} Also at Institute of Theoretical Physics, Ilia State University, Tbilisi; Georgia.
- ^{ai} Also at LAL, Université Paris-Sud, CNRS/IN2P3, Université Paris-Saclay, Orsay; France.
- ^{aj} Also at Louisiana Tech University, Ruston LA; United States of America.
- ^{ak} Also at Manhattan College, New York NY; United States of America.
- ^{al} Also at Moscow Institute of Physics and Technology State University, Dolgoprudny; Russia.
- ^{am} Also at National Research Nuclear University MEPhI, Moscow; Russia.
- ^{an} Also at Near East University, Nicosia, North Cyprus, Mersin; Turkey.
- ^{ao} Also at Ochanai Academic Production, Ochanomizu University, Tokyo; Japan.
- ^{ap} Also at Physikalisches Institut, Albert-Ludwigs-Universität Freiburg, Freiburg; Germany.
- ^{aq} Also at School of Physics, Sun Yat-sen University, Guangzhou; China.
- ^{ar} Also at The City College of New York, New York NY; United States of America.
- ^{as} Also at The Collaborative Innovation Center of Quantum Matter (CICQM), Beijing; China.
- ^{at} Also at Tomsk State University, Tomsk, and Moscow Institute of Physics and Technology State University, Dolgoprudny; Russia.
- ^{au} Also at TRIUMF, Vancouver BC; Canada.
- ^{av} Also at Università di Napoli Parthenope, Napoli; Italy.
- * Deceased.